Available online at www.sciencedirect.com
ScienceDirect
Journal of Volcanology and Geothermal Research xx (2008) xxx–xxx
Journal of volcanology and geothermal research
www.elsevier.com/locate/jvolgeores

Research paper

Contrasting styles of welding observed in the proximal Askja 1875 eruption deposits I: Regional welding

R.J. Carey [a,*], B.F. Houghton [a], T. Thordarson [b]

[a] Department of Geology and Geophysics, SOEST, University of Hawai`i, Honolulu, HI 96822, USA
[b] School of GeoSciences, University of Edinburgh, Edinburgh EH9 3JW, United Kingdom

Received 11 March 2007; accepted 9 November 2007

Abstract

Welded fall deposits on the northern caldera rim at Askja volcano are associated with the Plinian phase of the 1875 eruption. Two welding units occur within the proximal Plinian fall centered on stratigraphic sub-units which, where non-welded, are poorly sorted and ash-rich with high abundances of fluidal and needle-like ash particles. Welding has formed due to two discrete processes; a) the sintering of hot ash and lapilli which forms the two distinct units that are laterally continuous on distance scales of tens of meters (termed 'regional welding'), and b) creation of welding halos enclosing large, dense, discrete, non- to poorly vesicular spatter bombs that are up to 9 m in diameter (termed 'local welding'). This paper is concerned with the nature of regional welding and the companion paper (this issue) focuses on the phenomenon of local welding.

Three case studies documenting the range of welding patterns observed in regional welding are presented here. Vertical and lateral profiles of welding intensity, together with the deposit characteristics reveal that welding could only occur when the accumulation rates were sufficient and that grain size and thickness are second order factors facilitating welding. Rapid and reversible shifts in both thickness and welding grade are observed on a ~10 m scale laterally along the caldera rim suggesting considerable unsteadiness of the transport regime, which promoted localized fluctuations of the accumulation rate. The welded deposits prompt re-examination of both the dynamics of the Plinian phase of the 1875 eruption and the distribution of source vents. The dispersal of the welding units is not compatible with deposition from the full height of the Plinian plume. Similarly to the ultra-proximal deposits of Novarupta or Tarawera, these clasts probably fell from heights of hundreds of meters to <4 km, retaining sufficient heat to weld after deposition. The E–W elongated distribution of the welded units is also not compatible with a single source vent, and favors several vents that were in a fountaining phase, and located adjacent to the northern rim.

Keywords: Askja; welding; welded falls; Plinian

1. Introduction

Here we describe rhyolitic welded fall deposits from the 1875 eruption of Askja volcano. Welded deposits are located in two separate regions of the caldera; the south west corner and along the northern rim. The welded deposits on the northern rim are the focus of this paper (Fig. 1) and are unmistakably fall deposits, due to their mantling character and grain size characteristics. Welding at this location takes two forms; a) the sintering of hot ash and lapilli, which is then overprinted by b) welding halos enclosing large, dense, discrete spatter bombs up to 9 m in diameter. This paper is concerned with a) and a companion paper (Carey et al., in press) describes b).

1.1. Welding in pyroclastic rocks

Welded air fall deposits appear to be rare, as few examples are documented in the scientific literature (e.g. Sparks and Wright, 1979; Wolff and Wright, 1981; Turbeville, 1992) — most examples of welded deposits are associated with ash flow tuffs (Kamata et al., 1993; Quane and Russell, 2005; Sheridan and Wang, 2005). This literature describing welded air fall is generally restricted to deposits formed during mildly explosive

* Corresponding author. Tel.: +1 808 956 5960; fax: +1 808 956-5512.
E-mail address: beccarey@hawaii.edu (R.J. Carey).

0377-0273/$ - see front matter © 2007 Elsevier B.V. All rights reserved.
doi:10.1016/j.jvolgeores.2007.11.020

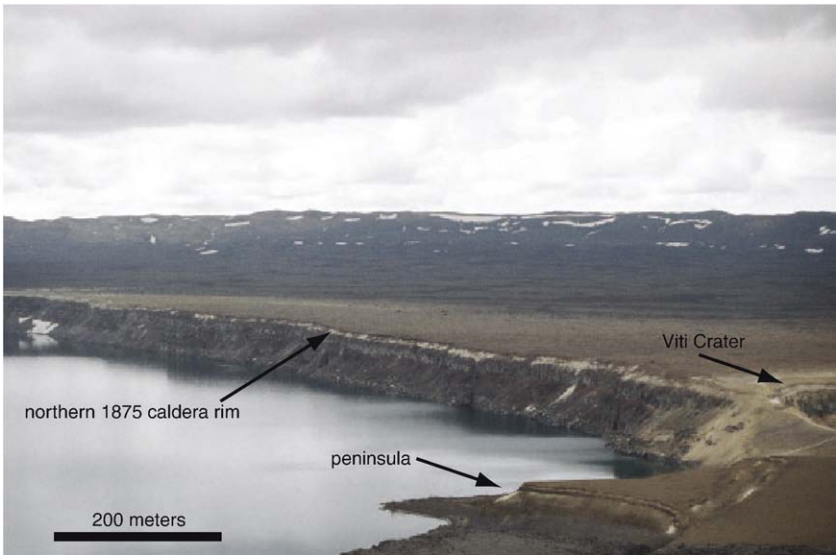

Fig. 1. The northern rim of the 1875 caldera in the foreground, now filled by Lake Öskjuvatn. The mountainous background is the western margin of the main Askja caldera. Note the position of Víti phreatic crater, used as a reference point throughout the text, and the peninsula, with 2 orthogonal faces. The welded deposits are red-colored distributed on the northern rim. (For interpretation of the references to colour in this figure legend, the reader is referred to the web version of this article.)

eruptions resulting in locally dispersed pyroclastic ejecta and restricted to the proximal environment <2 km from vent (Hackett and Houghton, 1985; Karhunen, 1988). Welded air fall deposits however are common products of many modern volcanoes in proximal regions and cover the full range of composition. Fall welded deposits of peralkaline composition (e.g., Pantelleria, Stevenson and Wilson, 1997; Mayor Island, Stevenson et al., 1993) and welded basaltic spatter deposits (e.g. Karhunen, 1988; Calderone et al., 1990) appear to be dominant and few examples of welded calcalkaline silicic air fall deposits have been documented (Sparks and Wright, 1979; Hackett and Houghton, 1985; Duffield, 1987). Examples range from basaltic through rhyolitic magma compositions and the best documented examples include the Thera and Therasia tuff from Santorini (dacite) (Sparks and Wright, 1979) and the Pinnacle ridge tuff from Ruapehu volcano (andesite) (Hackett and Houghton, 1985). The Askja 1875 welded fall deposits were identified and briefly described by Sparks and Wright (1979).

The process of welding of pyroclastic deposits has previously been described as the sintering together of hot, glassy pyroclastic fragments and their flattening under compactional load at temperatures above the glass transition temperature (e.g. Smith, 1961; Cas and Wright, 1987; Quane and Russell, 2005). Two important controls on welding are melt viscosity (which is dependant on temperature and composition) and lithostatic load (thickness of the deposit). Other parameters that control the final degree of welding in air fall deposits are eruption style (e.g. fountaining), emplacement temperature, accumulation rate, the composition of the magma, rate of crystallization, slope and lithic clast content. During the welding process, accumulation of hot, plastic pyroclasts forms layers of agglutinated to incipiently welded pyroclasts. Welding intensifies with higher accumulation rates, and under the compactional load of overlying tephra, changes will occur in the physical characteristics of the pyroclasts, such as plastic flattening and deformation of pyroclasts. Physical properties such as a reduction of primary porosity and increases in density accompany welding and can be used as quantitative measures of welding intensity (Quane and Russell, 2005).

The problem posed by all welded fall deposits is determining the conditions under which airborne ejecta can remain significantly hot during flight to weld and compact after deposition. The welding process is influenced by numerous depositional processes together with the inherent thermodynamic properties of the ejecta and deposit. Previous authors (e.g. Sparks and Wright, 1979; Head and Wilson, 1989) have suggested that accumulation rate is the critical factor, by covering and insulting clasts quickly and hence slowing cooling rates. In addition, Head and Wilson (1989) highlight that clast temperature on landing is another important factor, which is a function of both clast size and flight time. Thomas and Sparks (1992) completed a theoretical study combining estimates of clast cooling times with deposition rates from a Plinian column to postulate that grain size appeared to be the most important factor in facilitating welding. Recently Capaccioni and Cuccoli (2005) modeled cooling rates of particles during ballistic transport and deposition. These authors have also proposed that grain size is a critical factor in promoting welding or agglutination. Another key factor is deposit thickness which increases load pressure and slows heat loss and hence will promote higher degrees of welding (Quane and Russell, 2005).

1.2. General setting of Askja volcano

The central volcano Askja is situated on the southern sector of the Askja volcanic system and has been active for >200,000 years (Fig. 2) (Sigvaldason, 2002). It is the locus of

Please cite this article as: Carey, R.J., et al., Contrasting styles of welding observed in the proximal Askja 1875 eruption deposits I: Regional welding, J. Volcanol. Geotherm. Res. (2008), doi:10.1016/j.jvolgeores.2007.11.020

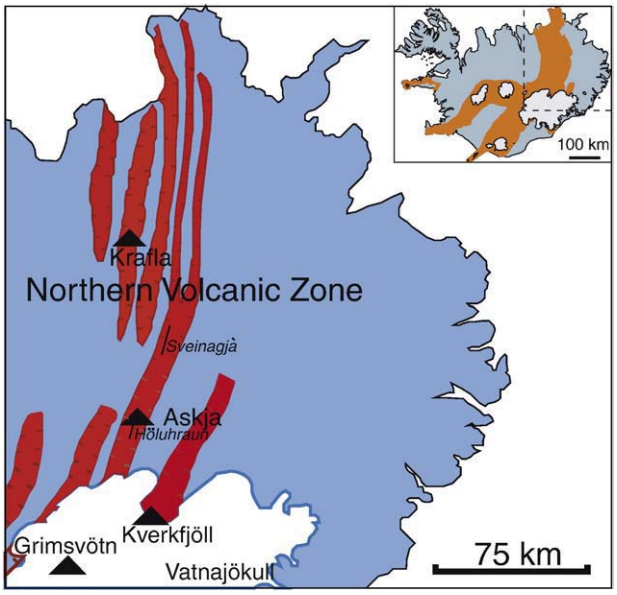

Fig. 2. Map of northeastern Iceland showing the volcanic systems of the Northern Volcanic Zone (NVZ) in red and the locations of associated central volcanoes shown with black triangles. Sveinagjá, 40 km north of Askja is the site of the precursory effusive event, producing 0.3 km^3 of basaltic lava which occurred between February and March 1875. Holuhraun, ~15 km south of Askja is a second site of basaltic precursors. Map modified from Sigvaldason (2002). (For interpretation of the references to colour in this figure legend, the reader is referred to the web version of this article.)

activity on the system and rises to more than 800 m above its surroundings, capped by the composite Askja caldera, which incorporates the nested 1875 Öskjuvatn caldera (Fig. 1). Two explosive silicic eruptions are known from Askja in Holocene times, the 1875 eruption and a ~10 ka event which has been estimated to be close to an order of magnitude larger (DRE volume 1.2 km^3; Sigvaldason, 2002). Askja is composed predominantly of basaltic hyaloclastites, pillow lavas erupted during subglacial times, and subaerial post-glacial lava flows which have partially filled in the main caldera. Nestled within this larger construct is the 230 meter-deep Öskjuvatn caldera, covering an area of 15 km^2. This structure formed during the 1873–1875 Askja volcano-tectonic episode due to post-1875 downfaulting and ring fracture collapse and is now occupied by Lake Öskjuvatn (Sigvaldason, 1979). Throughout postglacial times, activity at Askja has been vigorous with a number of basaltic eruptions on ring fractures surrounding the caldera rim. The recent activity appears to be controlled by lithospheric extension producing an en echelon array of north-northeast to south-southwest fissures on which are superimposed the main caldera ring fractures (Fig. 3). Post 1875 activity includes both explosive and extrusive eruptions of basaltic magma in 1921–22, 1929, 1931 and 1961 (Sigvaldason, 1979; Sparks et al., 1981).

Prior to the 1874–1876 volcano-tectonic episode, precursory activity began perhaps as early as 1867 (Thordarson et al., in preparation). Precursory activity that began in 1874 was due to rifting along the entire volcanic system, with eruptions at Askja central volcano, Sveinagjá 40 km north of Askja and Höluhraun, ~15 km south of Öskjuvatn on the fissure swarm (Fig. 2, Sigurdsson and Sparks, 1978a,b; Sigvaldason, 1979; Sparks et al., 1981, Thordarson et al., in preparation). Following the explosive subplinian–phreatoplinian–Plinian eruption in March 1875, post-eruption activity lasted into 1876 and included the phreatic creation of Víti crater on the northern rim of Öskjuvatn and continued weak

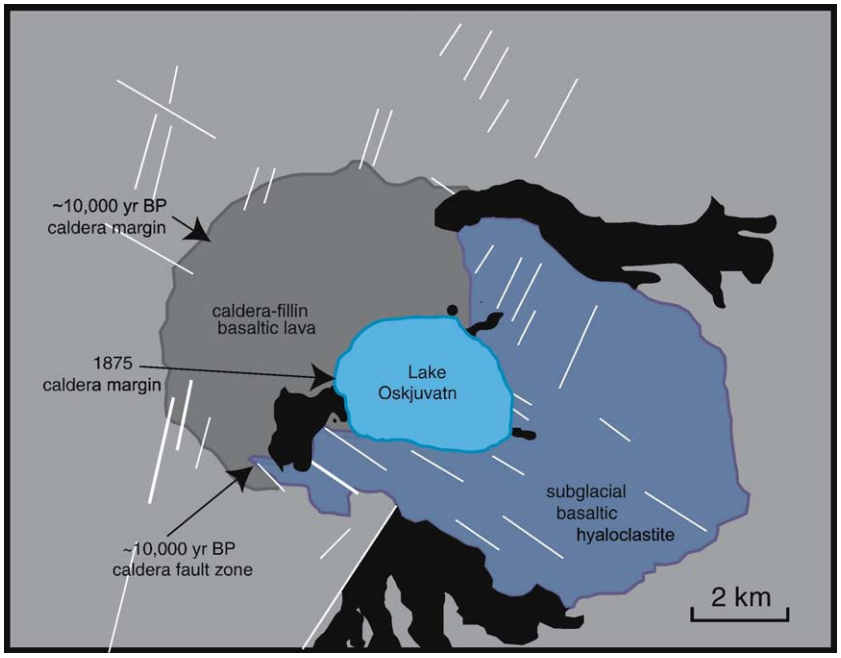

Fig. 3. Schematic map of the Dyngjufjöll central volcano, showing the main Askja and the nested 1875 (lake-filled) calderas. Tectonic lineaments form a cross-cutting pattern defined by SE–NW and SSW–NNE faults (white lines in figure). Eruptive activity in the Dyngjufjöll complex has predominantly occurred on these lineaments. Pre- and post-1875 basaltic activity has also occurred along ring faults that surround the 1875 caldera and main caldera rims in black. Diagram modified from Sigvaldason (2002). (For interpretation of the references to colour in this figure legend, the reader is referred to the web version of this article.)

Please cite this article as: Carey, R.J., et al., Contrasting styles of welding observed in the proximal Askja 1875 eruption deposits I: Regional welding, J. Volcanol. Geotherm. Res. (2008), doi:10.1016/j.jvolgeores.2007.11.020

phreatic activity in the southeast corner of Öskjuvatn (Sigvaldason, 1979; Sparks et al., 1981).

1.3. Previous work

The 1875 eruption produced a number of distinctive pyroclastic units, including non-welded subplinian, phreatoplinian and Plinian fall and pyroclastic surge deposits together with welded deposits erupted during the Plinian phase (Sparks and Wright, 1978; Sigvaldason, 1979; Sparks et al., 1981). Askja 1875 welded deposits have been previously described by Self and Sparks (1978), Sigvaldason (1979), Sparks and Wright (1979) and Sparks et al. (1981). Sparks and Wright (1979) describe two 1875 welded tuffs, located on the northern and southwestern rim of Öskjuvatn and formed during the main phase of the eruption in 1875, together with two welded fall deposits of Santorini. Sparks and Wright (1978) describe briefly the welded northern rim deposits but focus upon the welded deposits in the southwestern sector of the 1875 caldera.

1.4. The 1875 Askja eruption

The Askja pyroclastic deposits have been divided into six units (A–F) by Sparks et al. (1981). These units have been correlated with explosive activity between 1875 and 1876. The deposits of the main phase on 28–29 March, 1875 (Units B, C, D), comprise three distinct magmatic units, with a trend of fluctuating eruption intensity. These products were dispersed towards the east and cover a combined area of 628,000 km^2. Unit D is a very coarse grained, well sorted Plinian fall and is undeniably associated with the main fallout from the eruption. The welded deposits on the northern rim of the caldera are associated with the Plinian D phase of the eruption and are the focus of this paper.

2. The non-welded northern D deposits: stratigraphy and dispersal

The grain size, sorting, color and lithic abundances of non-welded sub-unit D deposits are often obscured when the deposits become welded. Here we describe these features and stratigraphic divisions within the non-welded deposits, to supply a framework to understand welding process.

2.1. Stratigraphy

The proximal unit D deposits, where non-welded, are separated into five sub-units, recognized to first order, by the alternating white and grey–brown coloration of each sub-unit (Fig. 4). Less striking but more reliable indicators of the stratigraphic boundaries between sub-units are shifts in grain size and componentry. We recognized that the grey–brown-colored D2 and D4 sub-units are coarse grained, poorly to very poorly sorted deposits with a higher abundance of ash than the D1/D3/D5 sub-units (20–30 modal%) and contain abundant fluidal ash particles. The non-welded characteristics have been used first to define and then to map stratigraphic boundaries

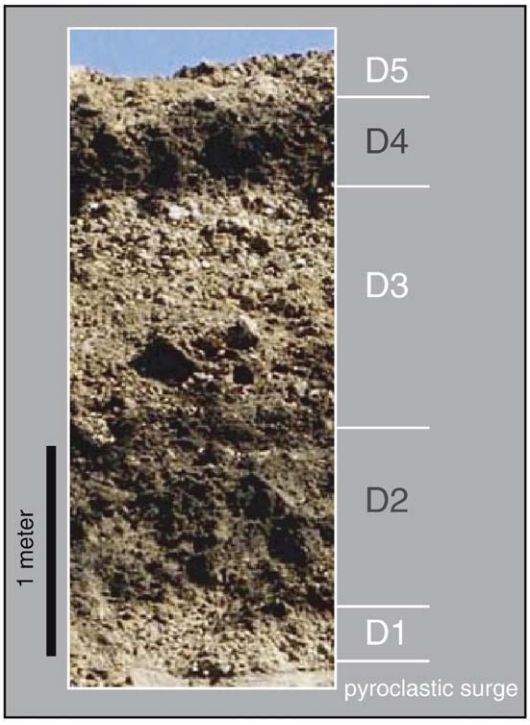

Fig. 4. The non-welded unit D stratigraphy with underlying unit C pyroclastic surge deposits, photograph taken at a proximal section on the peninsula (X_1 in Fig. 5). Note the color change between darker locally dispersed D2 and D4 deposits versus the lighter widespread D1, D3 and D5 sub-units. The boundaries between D1–D2 and D3–D4 are sharp, in contrast to the boundaries between D2–D3 and D4–D5.

between sub-units. The definition of five sub-units has enabled close stratigraphic correlations between sites and dispersal calculations within this proximal environment. The best area to quantify each sub-unit is immediately southeast of Víti crater, where a broad peninsula forms two orthogonal faces with continuous exposure of all the D sub-units (Fig. 5). Circumferential (NW–SE) outcrops and the peninsula (SW–NE) outcrops provides an opportunity to observe changes in thickness, grain size and componentry in a downwind–upwind transect (circumferential) and a crosswind (radial) transect (Fig. 5). On the downwind traverse, the D sub-units are largely non-welded except for the local influence of spatter bombs. On the cross wind traverse, the welding state of the deposits and the abundance of outsized spatter bombs in D2 and D4 increases significantly to the southwest, towards the tip of the peninsula. We measured ten sections on a NW–SE transect along a lower bench 50 m from the current lakeshore. A further four sections were measured on a NE–SW radial line along the upper bench of the caldera rim (Fig. 5). The following volcanological attributes of each sub-unit are defined below from those sections where welding is not present.

2.1.1. Sub-unit D1

Sub-unit D1 is the initial product of the Plinian D phase. It is a continuous layer around the caldera margin, however it cannot be distinguished from D3 when sub-unit D2 is absent. D1 is a white, coarse grained, poorly bedded, well sorted deposit consisting of

Please cite this article as: Carey, R.J., et al., Contrasting styles of welding observed in the proximal Askja 1875 eruption deposits I: Regional welding, J. Volcanol. Geotherm. Res. (2008), doi:10.1016/j.jvolgeores.2007.11.020

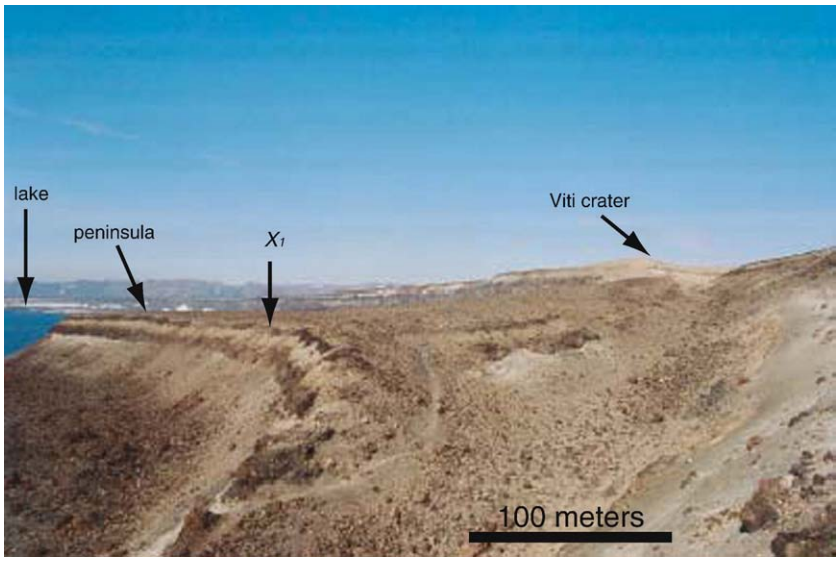

Fig. 5. Photograph of the peninsula near Víti, view to the west. The 1875 deposits mantle the peninsula and the alternation of light and dark sub-units of unit D is obvious. The northern rim is visible in the background. The SW–NE radial transect of four sections points into the lake, while the circumferential transect is the face perpendicular to this. Note the. X_1 is the section shown in Fig. 4.

highly to very highly vesicular pumice. The components are medium to coarse pumice lapilli and subordinate angular ash-sized shards. The lithic component is dominantly angular obsidian fragments; in abundance up to ~8 modal%. Bulk density measured in the field for the D1 sub-unit is 285 kg m^{-3}.

2.1.2. Transition between D1 and D2

The transition between D1 and D2 is recognizable due to a sharp decline in abundance of lithic clasts, an increase in maximum grain size, and the substantial increase in abundance of matrix, comprising predominately of fluidal juvenile clasts in the ash-sized fraction. D2 is typically darker in appearance; however, we also recognize a darkening of some D1 clasts, such that one single clast can have a cream-colored lower part and a dark brown upper part. This darkening phenomenon we interpret to be caused by oxidation from hot overlying D2 material.

2.1.3. Sub-unit D2

Sub-unit D2 is the lower of the two dark brown to grayish-black sub-units. It is consistently poorly to very poorly sorted and comprises fine to coarse lapilli and pumice bombs within a matrix of grey/brown ash, including fluidal particles, shards and needles. The matrix is fine to coarse ash and generally comprises 20–25 modal% of the sub-unit but reaches a maximum of 40 modal%. Four different lithic clast types are present, obsidian, granophyre, basalt and red-oxidized hyaloclastite clasts, and the total lithic abundance is consistently <2 modal%. The vesicularity of the pumice clasts is variable, although most are highly to very highly vesicular. Where it is thickest, we can define three parts within sub-unit D2. The lower part is dominated by dark grey clasts, and has high abundance of the ash-sized matrix (20–25 modal%). The middle part has a combination of dark and white to yellow/brown pumice clasts. The dark grey clasts dominate in the ash and block fractions and the abundance of the ash matrix is reduced to approximately 15–20 modal%. The white/cream/yellow clasts are not homogenous in color and can vary in one individual clast. The uppermost part is similar to the lowermost part in terms of components and ash matrix. Bulk density of the D2 sub-unit is 321 kg m^{-3}.

2.1.4. Transition between D2 and D3 sub-units

The exact transition between grey–brown-colored D2 and cream-colored D3 is difficult to identify due to the high abundance of brown/yellow oxidized clasts at the transition zone of the D2 and D3 sub-units. However an abrupt decrease in abundance of fluidal particles and ash content over no more than 5 cm presents an obvious marker.

2.1.5. Sub-unit D3

The proximal D3 deposits are widely dispersed, and merge with the D1 and D5 sub-units when D2 and D4 are missing, and together can be traced outside the caldera towards the east to form the bulk of the medial/distal fall unit that fell over eastern Iceland and Scandinavia. It is a white, clast-supported, coarse grained pumice lapilli and bomb deposit, which is moderately well sorted. The pumices are mostly highly vesicular with a very minor proportion of clasts that have breadcrusted exteriors. The sparse matrix (<10 modal%) within this sub-unit is dominantly pumice shards and fragments. The lithic clasts are predominantly obsidian, basaltic lava and granophyre fragments. The D3 sub-unit has a bulk density of 258 kg m^{-3}.

2.1.6. Transition between D3/D4

This transition is always sharp and linear. The distinction between D3 and D4 is straightforward, marked by a large and abrupt increase in maximum grain size, linked with increases in the abundance of matrix and appearance of fluidal ash-sized clasts. We do not observe any 'mixed layer', containing both light and dark clasts.

Please cite this article as: Carey, R.J., et al., Contrasting styles of welding observed in the proximal Askja 1875 eruption deposits I: Regional welding, J. Volcanol. Geotherm. Res. (2008), doi:10.1016/j.jvolgeores.2007.11.020

2.1.7. Sub-unit D4

Where non-welded, this sub-unit is a very poorly to poorly sorted layer, with abundant coarse bombs up to 80 cm in diameter. It is poorly bedded and contains up to 30 modal% ash matrix, which includes shards, needles and fluidal ash particles. The lithic clast content within this layer is low, ~0–2 modal%, and includes obsidian and granophyre lithic clasts. Juvenile clasts are highly to very highly vesicular pumice; approximately 20% of these clasts have very highly elongated vesicles and shiny blue exteriors. The bulk density of this sub-unit is 548 kg m^{-3}.

2.1.8. Transition between D4/D5

Similarly to the transition between sub-units D2 and D3, the D4/D5 transition is also difficult to identify on an outcrop scale due to the high abundance of brown/yellow oxidized clasts at the transition zone. The finer characteristics such as increase in lithic clast content and decrease in both the abundance of ash and fluidal ash components are better indicators of this transition.

2.1.9. Sub-unit D5

D5 is a poorly sorted sub-unit of fine to coarse pumice lapilli within an ash matrix (<10 modal%), with abundant coarse bombs resting on the upper surface. The matrix comprises white fine to coarse ash, including pumice shards, and fibrous fragments. The lithic content is approximately 10–15 modal%, the second highest after D1, and comprises fragments of obsidian, granophyre, basalt lava and red-oxidized hyaloclastite. This sub-unit cannot be clearly delineated from D3 where D4 is no longer present. The bulk density of this sub-unit is 282 kg m^{-3}.

2.2. Geometry and dispersal

The proximal deposits within the caldera are distributed in an elongated ellipse centered on lake Öskjuvatn and components of the proximal stratigraphy (sub-units D1, D3 and D5) merge into the widely dispersed medial Plinian D fall towards the east and northeast beyond the phreatic crater Víti (Fig. 6). In comparison, the dark sub-units D2 and D4 have a much more restricted dispersal, confined solely to the proximal environment along the northern rim of Lake Öskjuvatn (Fig. 6). The combined area of non-welded and welded D2 and D4 sub-units cover an area of 2.3 km^2, to be compared with an area of 4919 km^2 within the 2 cm isopach for the widespread Plinian D fall. Approximately 950 m east of the Víti crater, D4 becomes a discontinuous layer and a further 200 m away dark clasts and bombs are no longer present at this level in the stratigraphy. D2 follows a similar pattern, 1.3 km from Víti this layer is no longer continuous and at a further 300 m, D2 clasts are absent. At this point, D1, D3 and D5 cannot be distinguished one from another. For this reason we plot the combined thickness of these units in Fig. 7, which clearly shows the sharper downwind decline in thickness of D2 and D4 with respect to the enclosing sub-units. In this region the downwind linear thickness half-distances are: 5.9 km for the combined D1 +D3+D5 sub-units; 310 m for the lower dark sub-unit D2; and 70 m for the upper dark sub-unit D4. The light-colored sub-units

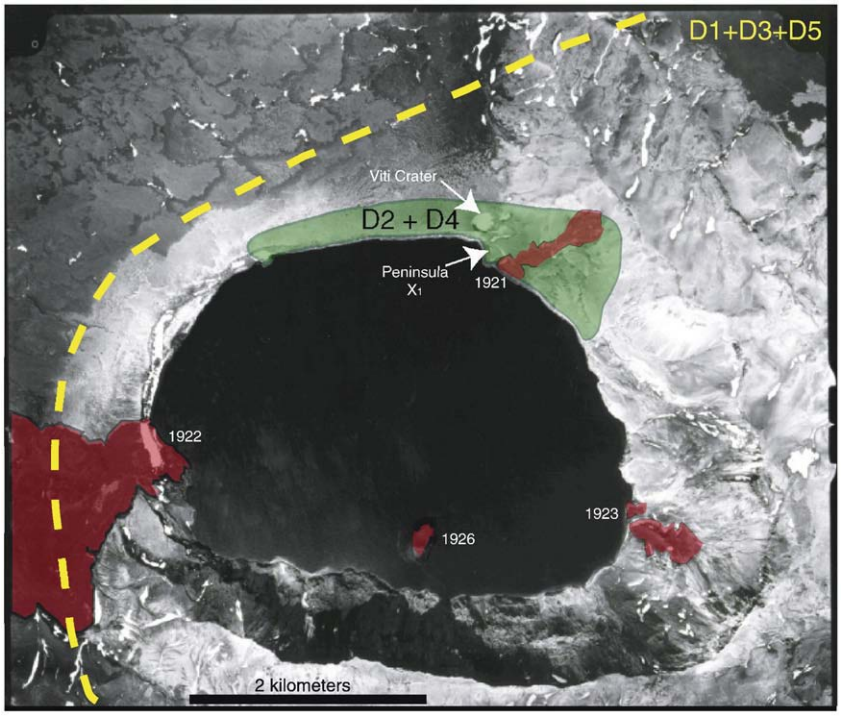

Fig. 6. Aerial photograph of the 1875 caldera with the outline of the disitributions of the locally (D2+D4) and widely dispersed (D1+D3+D5) sub-units. The white 1875 tephra is draped upon the basaltic hyaloclastite range from the northeast to southwest. To the north and west are the main caldera-filling lavas. Post-1875 activity is colored red, with the date when it was erupted. Note that the post-1875 activity is focused on ring fractures around the 1875 caldera. X_1 is the location of samples taken for grain size analysis for each sub-unit.

Please cite this article as: Carey, R.J., et al., Contrasting styles of welding observed in the proximal Askja 1875 eruption deposits I: Regional welding, J. Volcanol. Geotherm. Res. (2008), doi:10.1016/j.jvolgeores.2007.11.020

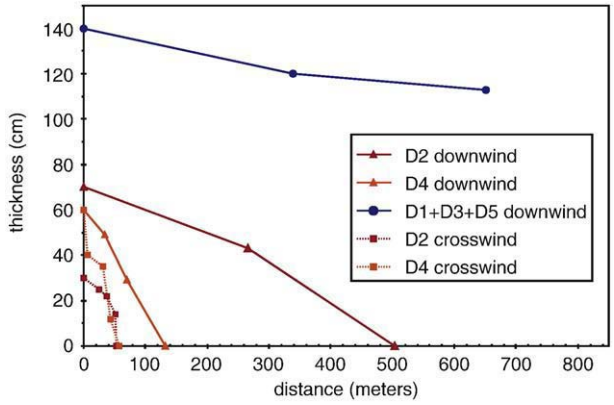

Fig. 7. Plot of downwind and crosswind thinning for the widespread Plinian sub-units (D1+D3+D5) versus the locally dispersed sub-units (D2+D4). The D2 sub-unit is more widely dispersed downwind than its D4 counterpart. Downwind thinning half-distance for D1+D3+D5 is 5.2 km, and the values for D2 and D4 are 312 and 70 m respectively. The crosswind thinning half-distances for D2 and D4 are 45 and 33 m respectively.

are thus one to two orders of magnitude greater in dispersal than the dark-colored sub-units. In addition, D2 has a downwind dispersal five times greater than D4. D2 is also more widely dispersed crosswind than D4 as shown on a plot of radial linear thickness half-distance (Fig. 7).

2.3. Grain size and componentry

In order to quantify grain size of proximal deposits from the main Plinian phase, samples were collected from a section on the peninsula where all the deposits are entirely non-welded (site X_1 on Figs. 5 and 6). This site was chosen as it represents the proximal grain size of each sub-unit and is the most proximal section where all sub-units can be observed. Grain size samples were taken from each sub-unit and the weight of the largest clast was measured and used to determine an approximate size for a representative sample. All sub-units were sieved and weighed in the field down to -4φ (16 mm) and a representative split of the <16 mm fraction was taken to the laboratory for further analysis. Proximal grain size results for each sub-unit are shown in Table 1. The median grain size of the sub-units shows a coarsening with stratigraphic height. There is a three times increase in median grain size from D1 to D2, and smaller changes of medial grain size between other sub-units (Table 1). In terms of sorting, the dark sub-units D2 and D4 have Inman (1952) sorting values (σ_φ) between 3.3 and 2.5 and are poorly sorted. D1 is also poorly sorted (2.5) and D3 and D5 are better sorted (1.7 and 2.1 respectively). Relative to 'dry' fall deposits in Walker (1971), the D2 and D4 samples, while still unimodal, show significantly poorer sorting. Similar samples documented by Walker (1971) show σ_φ values dominantly between 0.7 and 2.0.

3. The welded D deposits

3.1. Background to study of the welded D deposits

The welded deposits described here are restricted to the northern caldera rim. Proximal to the northern rim welding is most intense and decreases in intensity non-uniformly outward. Smaller areas of welding are also observed near Víti and on the peninsula. The fundamental nature of the welding process and its characteristics are similar for each of these regions. Here we describe the nomenclature used for the observed degrees of welding and the techniques applied during this study.

Table 1
Table of median diameter (Md_φ) and Inman sorting coefficients (σ_φ) for each sub-unit within the unit D deposits. Note the increase of median grain size with time and the poor sorting of D1, D4 and especially D2. In comparison the D3 and D5 sub-units which contribute mostly to the widespread Plinian fall are better sorted

Sub-unit	Md (φ)	S.D. (σ_φ)
D1	−3.2	2.5
D2	−4.7	3.3
D3	−5.3	1.7
D4	−5.9	2.5
D5	−6.1	2.1

3.2. Nomenclature for describing welded air fall pyroclastic deposits

In the literature, the nomenclature used for describing welded pyroclastic rocks and the degree of welding varies for welded ignimbrites (e.g. Sheridan and Ragan, 1976; Quane and Russell, 2005) and welded fall deposits (e.g. Sparks and Wright, 1979; Wright, 1980). For fall deposits, the terminology also varies for spatter deposits versus welded fall deposits of predominantly pumice (Sparks and Wright, 1979; Karhunen). Recently Quane and Russell (2005) have proposed a quantitative classification of welding intensity for ignimbrites, based on physical attributes of bulk density, porosity, uniaxial strength, and measurements of clast dimensions. Here we outline a similar classification scheme for describing welding intensity, from non-welded to densely welded, for the Askja air fall deposits (Table 2). These terms for welding intensity are based on measurable attributes of both

Table 2
Nomenclature used in descriptions of welding intensity of the Askja 1875 welded deposits. For each welding grade, attributes of both clasts and matrix are described

Welding grade	Attributes of welding	
	Matrix	Clasts
Densely	Glassy matrix, no obvious pyroclastic texture	Ghost-like outlines of clasts with minor relic vesicularity
	No void space between clasts	Extremely flattened fiamme
Moderately	No void space between clasts, matrix texture	Elongated clasts with flattened vesicles, outlines of clasts
	No longer apparent, eutaxitic textures	Still recognizable, some relic vesicularity of clasts
Slightly	Clasts sintered together, however clastic texture	Firmly sintered edges, flattened clasts
	Still apparent, void space present	Edges of clasts still partly recognizeable
Tack	Loose, unconsolidated with void space	Sintered edges, ragged form of pumices
		Rounded undeformed vesicles
No welding	Loose, unconsolidated	Undeformed, original ragged form of pumices

Please cite this article as: Carey, R.J., et al., Contrasting styles of welding observed in the proximal Askja 1875 eruption deposits I: Regional welding, J. Volcanol. Geotherm. Res. (2008), doi:10.1016/j.jvolgeores.2007.11.020

clasts and matrix. Clast flattening, shape, vesicle geometry and vesicularity were observed, together with matrix cohesiveness, texture and vesicularity.

3.3. Methods

At each section photographs were taken together with sketches and a detailed stratigraphic log describing thickness, color, ash content, grain size, sorting, lithic abundance and degree of welding. When recording the thickness of regional welding along the northern rim and peninsula, measurements were taken only in places where there were no spatter bombs in the immediate area (~1 m in either direction to avoid the thermal overprinting by these bombs). The welding state was recorded at every location where the thickness was measured.

3.3.1. Clast aspect ratio and density

The welding intensity of pyroclastic deposits can be quantified by changes in fabric and texture as well as measurements of physical properties such as clast aspect ratio, density and porosity. These properties can vary both vertically and laterally.

3.3.1.1. Aspect ratio. Aspect ratio measurements were made from five clasts at each site which appeared most representative of the general clast population. The X and Y axes were measured perpendicular to each other and the degree of welding was noted, together with descriptions of clast morphology (spatter vs. pumice).

3.3.1.2. Density sampling. Bulk rock density samples were taken from the welded deposits with a chisel and hammer. Care was taken to collect samples over very narrow intervals that represented a specific grade of welding intensity. Spatter bombs, if present in the field sample, were removed from the laboratory sample so not to bias the data towards high density values.

3.3.2. Calculations of deposit pre-welded thickness

To investigate the effect of pre-welding thickness on welding intensity we collected density samples from each welding zone at every section, assumed values for the bulk density of non-welded material and applied the following expression to determine pre-welding thickness from the reduction in density:

$$L_0 = L_w\left(\frac{\rho_w}{\rho_0}\right)$$

Where L_0 is the original thickness, L_w is the present thickness, ρ_w is the density of the sample and ρ_0 is the bulk density of non-welded material.

We calculated a bulk density of non-welded D4 material based on the percentages of components in the basal non-welded D4 layer and using an average density value for the constituent pumice clasts, derived from density measurements of 100 clasts in the 16 mm size fraction from an adjacent D4 deposit.

Our mixture comprises the following: 48% pumice lapilli with a pumice density of 357 kg m^{-3}, 30% ash with a bulk density of 1100 kg m^{-3}, 20% interstitial pore space in open void spaces between lapilli and 2% lithic clasts with a density of 2350 kg m^{-3} to result in a non-welded D4 bulk density of 548 kg m^{-3}.

3.4. Diversity and nature of welding — general

A key feature of the northern welded D2 and D4 deposits is rapid changes in welding state, which can be observed along horizontal distances of less than 100 m. We have identified two distinctly different processes which led to welding; i) relatively uniform compactional adhesion and sintering of ash and lapilli, and ii) local flattening and heating of the matrix by large discrete spatter bombs which range in size up to 9 m and decrease in abundance radially outboard of the caldera rim. The focus of this paper is the first style of welding, termed regional welding. However for clarity, we wish to introduce here the second style of welding which we call local welding (Fig. 8). Local welding is described fully, with case studies in Carey et al. (in press). Regional welding is defined by consistent intensities of welding (irrespective of proximity to large clasts), which are maintained on distance scales of at least tens of meters. Regional welding at the northern rim involves comparatively uniform adhesion and weak flattening of ash and lapilli to yield mostly tack-and-slightly welded deposits. Only rarely have we observed moderately welded material. Within regional welding we observe clasts with flattening ratios of 1:2 to 11:1 but commonly values are between 2:1 and 5:1. Densities taken from regionally welded samples yield results between 650 kg m^{-3} and 1620 kg m^{-3}. This style of welding is somewhat simpler to interpret than local welding (Fig. 8). Local welding is due to large discrete spatter bombs impacting into, compressing and supplying heat to an asymmetrical halo of surrounding material, which then undergoes softening, flattening and sometimes even rheomorphic flow. This material may have been previously non-welded (e.g., parts of sub-unit D3 in proximity to spatter bombs) or may have had some component of regional welding.

3.5. Welding units

We have devised a welding nomenclature to represent the two welded units we observe in the field. These welding units are centered upon but not limited to sub-units D2 and D4. Thus the welding units are not coincident with stratigraphically defined sub-units and we name them W1 and W2, centered on D2 and D4 respectively. At a limited number of sections, W1 falls entirely within D2 and W2 within D4; however at most sections W1 can encroach into D1 and/or D3 and W2 into D3 and/or D5. This nomenclature exists independent of the styles of welding that have contributed to the welding. For example, W1 can reflect purely regional, regional and local (Fig. 8), or less commonly, simple local welding (Fig. 8).

4. Regional welding

4.1. Documentation of background welding — vertical and lateral changes

4.1.1. Distribution of non-welded D2 and D4 deposits

The sub-units on which welding is centered, D2 and D4, have a much more restricted dispersal than the Plinian D1, D3 or D5 deposits, and have contrasting dispersals (Figs. 6 and 7). In

Please cite this article as: Carey, R.J., et al., Contrasting styles of welding observed in the proximal Askja 1875 eruption deposits I: Regional welding, J. Volcanol. Geotherm. Res. (2008), doi:10.1016/j.jvolgeores.2007.11.020

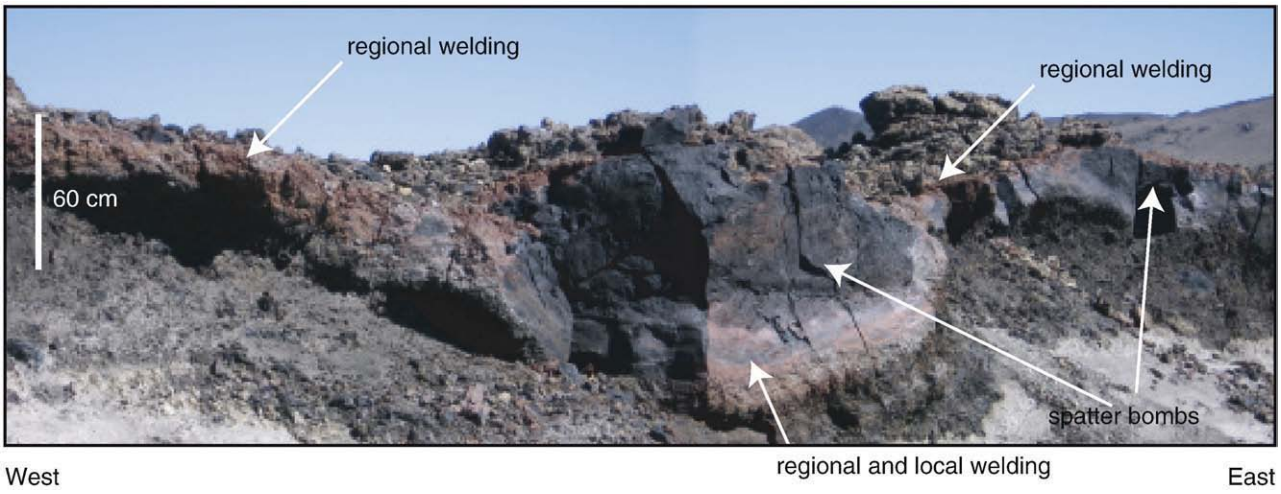

Fig. 8. Photograph illustrating both types of welding observed in the 1875 welded deposits — regional welding and local welding. Regional welding forms a continuous protruding welded bench, which has been deformed due to the arrival of meter-sized spatter bombs. Local welding is easy to identify due to its close proximity to spatter bombs. At this site the thickness of regional welding is approximately 30 cm, whereas the locally welded deposits concentric around the large spatter bomb are 55 cm-thick, and formed at the expense of formerly non-welded D3+D4 material. This spatter bomb in the foreground is ~1.9 m×95 cm.

particular, D2 extends further to the south east along the caldera margin than D4, but does not extend as far to the east. D4 does not extend as far west along the northern caldera rim as D2 (Fig. 9a and b).

4.1.2. Lateral distribution of W1 and W2 regional welding

Regional welding is common to both welding units; however, these units and their associated non-welded equivalents (D2 and D4) have contrasting distributions. (Fig. 9a and b). In particular the distribution of W2 is slightly skewed to the west with respect to W1. The extent along the northern rim of regional welding is approximately the same for the two units; however the area covered is less for W2, mainly a more limited radial extent.

4.1.2.1. Welding unit 1. W1 is centered on the central-west portion of the northern caldera rim (Fig. 9a). The lateral extent is approximately 1.15 km along the rim and its radial range outward of the rim is, at maximum, 50 m. The area covered by this welding unit is 0.18 km^2. At the eastern but particularly at the western limit of this welding unit, we observe patchy non-continuous welding (Fig. 9a). Welding can develop and vanish over lateral distances of ~10 m with non-welded D2 material intervening. At the eastern end, we observe ~50 m of such discontinuous welding, prior to a gap of ~100 m of non-welded material before continuous welding appears again. At the western end we observe discontinuous welding for 240 m, for intervals from ~10 m to 50 m. There appears to be no pattern in the frequency or length of these welded intervals.

4.1.2.2. Welding unit 2. W2 is focused on the central and eastern portions of the northern caldera rim (Fig. 9b) and its extent along the northern rim is 1.24 km. It overlaps with W1, so that at many sections along the rim, both regionally welded W1 and W2 are present (Fig. 9a and b). The area covered by W2 is 0.20 km^2. At the eastern margin of W2, there is a discontinuous zone of welding that extends outwards for a further 115 m (Fig. 9b). Stratigraphic sections described in case study 1 (Section 4.2), are within this zone. This eastern discontinuous zone is much greater than the analogous discontinuous zone on the western margin. This western discontinuous zone extends for only 85 m and is defined by only two zones of welding that are 20–40 m wide.

4.1.3. Lateral changes in thickness

In both welding units, we observe rapid changes in thickness over short lateral distances (Fig. 9a and b). We have made thickness measurements for strictly regional welding of both units along their entire lateral extents. We avoided areas where spatter bombs influenced the welding pattern.

4.1.3.1. Welding unit 1. W1 has two thickness maxima; the eastern maximum is between 760 and 890 m from Víti and the western maximum is between 1100 and 1310 m from Víti (Fig. 9a). Both have thickness maxima of 30 cm (Fig. 9a). On a range of scales, thickness and welding maxima appear to be decoupled. At the onset of continuous welding from the east, W1 shows a steady increase in thickness to the first maximum of 30 cm without an increase in the grade of welding. Within the interval of the thickness maximum, the welding grade does increase from tack to slight welding. Between the eastern and western thickness maxima, there is a significant decrease in thickness of the unit, which does not correlate with the observed changes in welding grade. To the west of the western maximum, W1 decreases rapidly and discontinuous zones of slight and tack-welding begin. These discontinuous zones show a general decrease in thickness with distance to the west, but values can vary by up to 20 cm over very short lateral distances of tens of meters.

4.1.3.2. Welding unit 2. W2 shows a uniform increase in thickness with small fluctuations over a distance scale of ~100–200 m to reach thickness maxima of 30 cm at distances of 550 to 610 m and 860 to 1050 m to the west of Víti (Fig. 9b). These

Please cite this article as: Carey, R.J., et al., Contrasting styles of welding observed in the proximal Askja 1875 eruption deposits I: Regional welding, J. Volcanol. Geotherm. Res. (2008), doi:10.1016/j.jvolgeores.2007.11.020

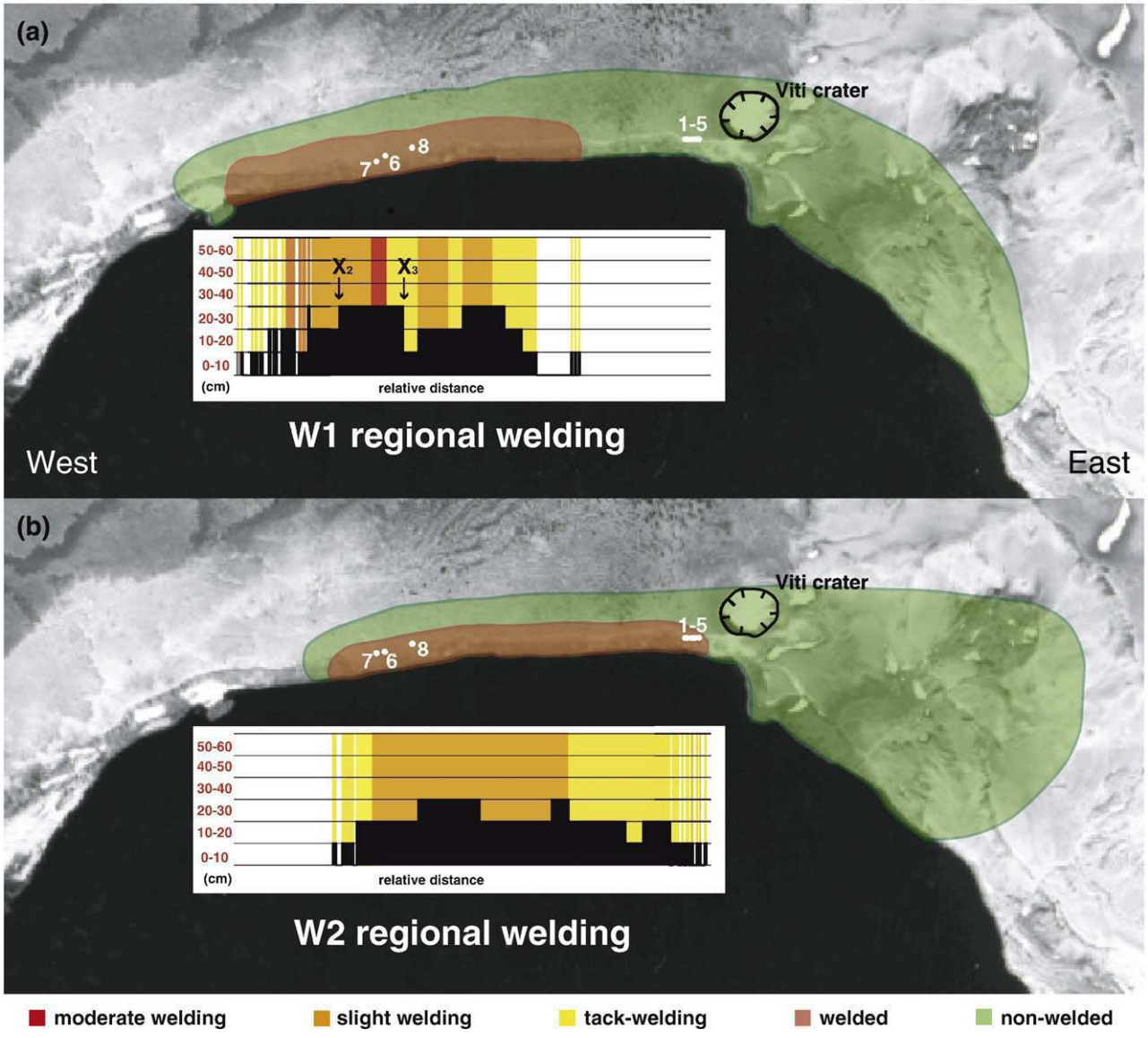

Fig. 9. a, b: The northern caldera rim, with the outlines of the distribution of non-welded D2 and D4 sub-units (green) and welded W1 and W2 units (red). The graph underneath is geo-registered with the aerial photo, showing the grade of welding and its thickness in centimeters for particular regions on the northern caldera rim. D2/W1 is shown in (9a) and D4/W2 is shown in (9b). Numbers refer to sections described in the text. The diameter of Víti crater is approximately 190 m, for scale. These graphs together show the lateral changes of degree of welding and thickness for the welding units. Note the simpler pattern of welding for the W2 unit with two thickness maxima. The W1 welding unit is more complicated with reversals of welding grade and significant thickness changes over very short lateral intervals. Víti crater is shown in black. Note the contrasting dispersals of non-welded D2 and D4. (For interpretation of the references to colour in this figure legend, the reader is referred to the web version of this article.)

thickness maxima correspond to the maxima in welding grade; however the maximum welding grade extends over a much greater distance than the thickness maxima. West and east of the thickness maxima, there is a gradual decrease of thickness paralleled by a decrease in the welding grade.

4.1.4. Lateral changes in maximum welding grade

Along the northern rim, there are non-systematic shifts in welding intensity, with rapid and reversible shifts over short lateral distances.

4.1.4.1. Welding unit 1. The maximum welding grades for W1 follow a systematic increase from tack-welding at the margins of the welding unit to slight to moderate welding grades in central portions of the unit (Fig. 9a). The onset of welding at the eastern end of W1 is consistently tack-welding as opposed to the western end where the regional welding is variable and patchy with alternating intervals of tack and slight welding present. Slight and tack-welding are equally common throughout the unit and it is common to see lateral reversions of welding grade. The maximum for welding grade is between 1160 and 1200 m west of Víti. The transition to this welding maximum is sharp. A change laterally from tack to moderate welding occurs on an east to west traverse over < 10 m, without a change in thickness. To the west of the W1 welding maximum, slight welding of the deposits continues for 290 m, in both laterally continuous and discontinuous intervals. Two other intervals of slight welding occur at 800 and 890 m and 950 to 1050 m.

Please cite this article as: Carey, R.J., et al., Contrasting styles of welding observed in the proximal Askja 1875 eruption deposits I: Regional welding, J. Volcanol. Geotherm. Res. (2008), doi:10.1016/j.jvolgeores.2007.11.020

The western interval corresponds to an increase in thickness of the W1 unit, while the other exhibits no correlation. Across the discontinuous zone, there is a gradual drop in maximum welding intensity towards the west.

4.1.4.2. Welding unit 2. W2 has a much simpler welding pattern. From the east, there is a gradual increase of welding grade from tack to slight welding (Fig. 9b). This tack-welded zone lasts for 340 m and the ensuing slight welding zone continues for a further 650 m. The zone of slight welding overlaps with the two 30 cm thickness maxima despite a drop of thickness to 20 cm in between. There is a much more restricted and discontinuous zone of tack-welding on the western portion of W2.

4.1.5. Changes of grain size along the northern rim

Grain size was recorded along the northern rim in an attempt to identify whether the increases in welding grade correspond to changes in grain size. These observations suggest that local changes in grain size lead to changes in the welding state. We consider this possible correlation in grain size and welding grade, and the smaller scale fluctuations in welding intensity in more detail via three case studies which describe the lateral onset of W2 regional welding, and welding maxima for W1 and W2 respectively.

4.2. Case study 1: the lateral onset of regional welding

The exposures along the northern rim record both the western and eastern onsets of regional welding for the W1 and W2 units. Regional welding of the W1 and W2 units is laterally displaced such that regional welding of W2 begins before the onset of W1 welding on an east to west traverse. The opposite is true in the west; the onset of W1 occurs prior to W2. In addition, the onset of welding on both margins of W1 and W2 is typically patchy and discontinuous over distances scales of tens of meters. Here we describe the onset of regional welding of the W2 unit on the eastern side as an example of this phenomenon.

W2 welding is first present on the north eastern sector of the northern rim, 80 m west of Víti. We have logged W2 at five locations along a 57-meter traverse to show lateral changes in thickness and degree of welding (Fig. 10). The lateral coverage of regional welding is patchy and non-uniform in terms of increases in both unit thickness and/or welding intensity. East of section 1 welding is absent and within 10 m to the west of section 5, regional welding becomes essentially continuous over lateral distances of 30–40 m. The welding recognized along this traverse is strictly regional and related to the adhesion and sintering together of lapilli and ash particles in the absence of heat contributions from large spatter bombs.

4.2.1. Section 1

At the easternmost section (1) the D4 layer including W2 is 60 cm-thick (Fig. 10). It can be separated into a non-welded basal layer, a welded unit (W2) and an upper non-welded layer. The basal non-welded layer of D4 (17 cm) is brown to black in color, moderately to poorly sorted; the ash matrix is dominated by juvenile fluidal ash particles including ash shards and needles comprising 40%. Above this layer, W2 is 17 cm-thick, has an abundant ash matrix (up to 30%) with diverse ash particles including fluidal clasts. W2 can be separated into two zones based on welding intensity, varying up to 10 cm in thickness along strike. The lower 7 cm is tack-welded, i.e., clast edges are lightly sintered together but there is no deformation of the clasts (density = 1130 kg m^{-3}; AR 1:1–3:1).

The upper 10 cm is slightly welded and the edges of clasts adhere and the fragments are slightly deformed but the matrix texture is still apparent (density = 1470 kg m^{-3}; AR 2:1

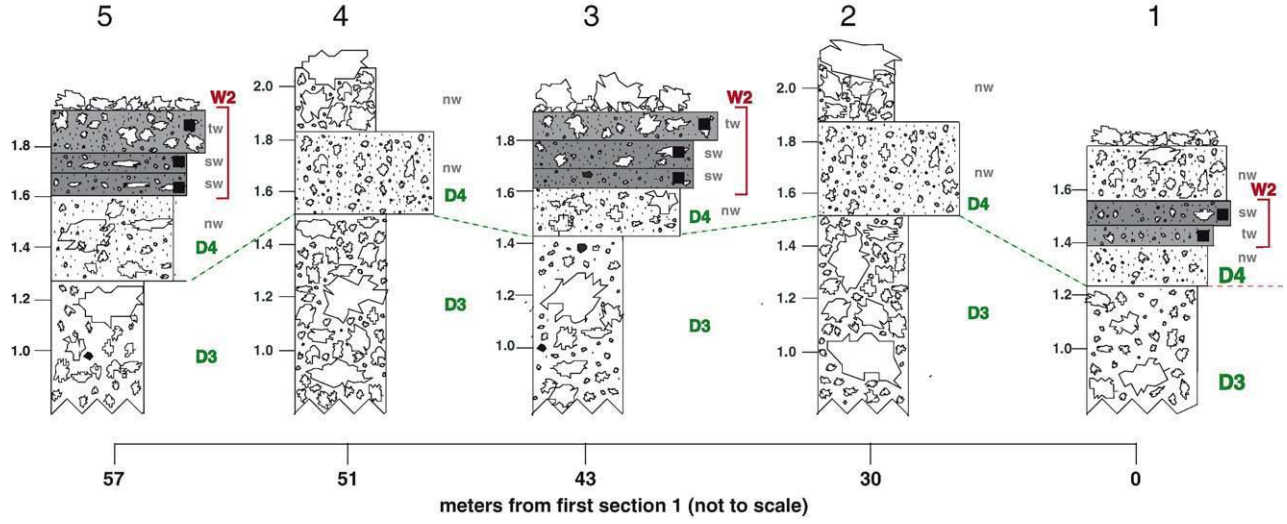

Fig. 10. Five sections measured at the eastern margin of W2. Note the fluctuations in the degree and thickness of welding over short lateral distances. Grey tones represent different degrees of welding in W2. The letters next to the sections represent the assigned welding grades as defined in the field: non-welded (nw), tack-welded (tw) and slightly welded (sw). The letters in green denote the non-welded stratigraphic nomenclature. (For interpretation of the references to colour in this figure legend, the reader is referred to the web version of this article.)

Please cite this article as: Carey, R.J., et al., Contrasting styles of welding observed in the proximal Askja 1875 eruption deposits I: Regional welding, J. Volcanol. Geotherm. Res. (2008), doi:10.1016/j.jvolgeores.2007.11.020

to 5:1). Above this zone is a non-welded, matrix-rich top that is 20 cm-thick.

4.2.2. Section 2

Section 2 is 20 m to the west of section 1 (Fig. 10). D4 is ~35 cm-thick, and is a poorly sorted, matrix-supported deposit that is non-welded throughout with clasts up to 6 cm and fluidal and needle-shaped ash particles which sometimes make up 25–30 modal% of the entire layer. The transition between D4 and D5 is well defined, but the occasional coarse D4 bomb protrudes through D5, which is ~15–20 cm-thick and comprises coarse ash to medium lapilli that are predominantly (~75%) light in color, in a coarse ash matrix comprising of pumice shards.

4.2.3. Section 3

The non-welded base to D4 is 19 cm-thick at section 3 (Figs. 10 and 11). The W2 unit is 29 cm-thick with a similar abundance of ash matrix to that of lower D4; however, median grain size increases with height. W2 can be separated into three zones. The lower zone is 8 cm-thick and slightly welded (density 1470 kg m^{-3}) with an abundant red oxidized ash matrix and fine lapilli up to 2 cm in diameter. Clasts are slightly elongate (AR 2:1 to 4:1) but with mostly equant vesicles. The middle zone (11 cm) is also slightly welded (density 950 kg m^{-3}) and red oxidized with abundant ash matrix and coarse lapilli up to 8 cm in diameter. This zone has a slightly greater degree of lapilli-flattening than the lower zone with aspect ratios between 3:1 and 6:1. The upper tack-welded zone (10 cm) consists of coarse ash, fine to coarse lapilli and bombs up to 12 cm in diameter, which are lightly sintered, with clast aspect ratios generally less than 2:1 (density 840 kg m^{-3}). On top of W2 is a scatter of 10–80 cm pumice clasts (D4+/−D5) which has been stripped of original matrix and now consists of ragged lapilli and bombs infiltrated by Víti mud.

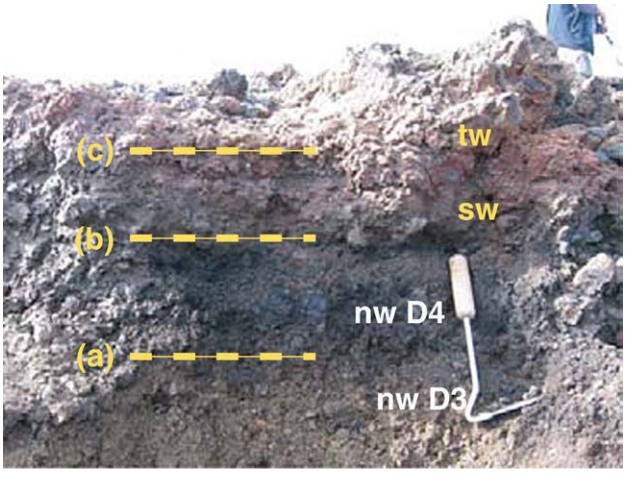

Fig. 11. Section 3 at the eastern onset of welding of the W2 unit. The boundary between D3 and D4 (a) can be easily recognized by the color change and sharp increase in ash within the matrix of D4. The vertical sharp onset of slight welding at this section (b) is also easy to recognize due to the protruding red oxidized bench. The transition between slight (sw) and tack-welding (tw) is shown at (c). (For interpretation of the references to colour in this figure legend, the reader is referred to the web version of this article.)

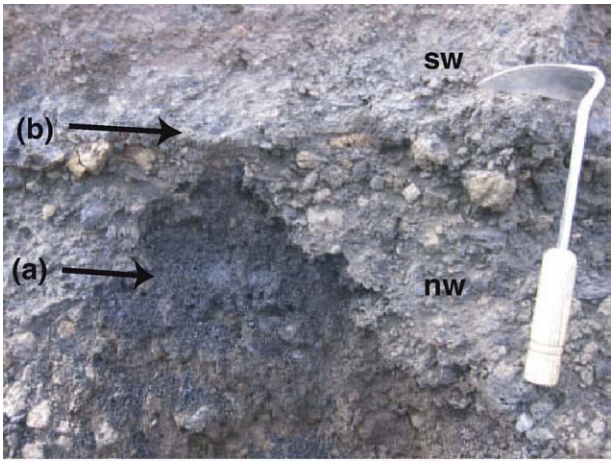

Fig. 12. The lower portion of section 5. Note the fine grain size of D4 (a) which also includes fluidal ash-sized particles and the sharp onset of slight welding allowing the deposit to form a protruding welded bench (b). Tool is 25 cm for scale.

4.2.4. Section 4

D4 is non-welded throughout section 4 (Fig. 10). D4 is 31 cm, matrix-supported (~35 modal%), and is poorly sorted. Particles range from fine ash to rare 8 cm clasts but more typically to 2–4 cm. The transition between D4 and D5 is conspicuous with a sharp decline in abundance, and a color change, of the ash components, and an increase in median grain size.

4.2.5. Section 5

At section 5, D4 and W2 have a combined thickness of 69 cm (Fig. 10). W2 is 35 cm and divided into three zones. The two

Table 3a
Table of the welded and calculated pre-welding thicknesses for each zone within sections 1–5. Using a calculated bulk density (548 kg m^{-3}) for the original nonwelded D4 material and density measurements collected from each welded layer, the prewelding thicknesses were calculated

	Section				
	5	4	3	2	1
Measured thicknesses (cm)					
Upper non-welded D4	0		0		20
Tack-welded	18		10		
Slightly welded	7		11		10
Slightly welded	10		8		
Tack-welded	0	0	0	0	7
Non-welded D4	34	31	19	35	17
Total (cm)	69		48		54
Total welded (cm)	35		29		17
Pre-welding thickness (cm)					
Upper non-welded D4	0		0		20
Tack-welded	34		15		0
Slightly welded	16		19		27
Slightly welded	27		21		0
Tack-welded	0				14
Non-welded D4	34		19		17
Total (cm)	111	31	75	35	78
Total welded (cm)	77		56		41
Welded thickness change (cm)	42		27		24
% Pre-welding thickness	62		64		69

Please cite this article as: Carey, R.J., et al., Contrasting styles of welding observed in the proximal Askja 1875 eruption deposits I: Regional welding, J. Volcanol. Geotherm. Res. (2008), doi:10.1016/j.jvolgeores.2007.11.020

Table 3b
Density values (kg m^{-3}) from zones in sections 1-5 used for calculations of the pre-welding thickness from sections 1 through 5. Sections listed in geographical order

Welded zone	Section				
	5	4	3	2	1
Upper non-welded					
Tack-welded	1030		840		
Slightly welded	1250		950		1470
Slightly welded	1490		1470		1130
Tack-welded					
Lower non-welded					

lower zones (in total 17 cm) are slightly welded and well delineated from the lower non-welded D4, due to a sharp transition of welding intensity and smaller clast sizes (Fig. 12). The slightly welded zones (densities 1490 kg m^{-3}, 1250 kg m^{-3}) are red-oxidized and the lapilli are only slightly elongate (AR 2:1), and the matrix texture is clear. The upper unit is tack-welded (density 1030 kg m^{-3}; AR 1:1–2:1) and features a red oxidized matrix.

4.2.6. Welded and non-welded thickness

The density measurements and pre-welded thicknesses of these five sections are summarized in Tables 3a and 3b respectively. The combined thickness of non-welded and welded D4 deposits in the welded sections range between 48 and 69 cm, whereas the non-welded sections have a more restricted thickness of D4 deposits, ranging from 31 to 35 cm. There is no systematic trend of changing thickness of individual zones, irrespective of which zones are included in the comparison. For example, the thickness of the non-welded basal D4 layer is non-uniform with distance along the traverse; the combined thickness of non-welded and welded deposits is also not uniform with distance and finally, it is difficult to correlate the thickening of the non-welded D4 part to the thicknesses of the probable D4 deposits in the welding sections. The thickness of the non-welded D deposits above the welding unit also varies between sections. At the westernmost sections, there is <10 cm of material above the welding unit. At section 1 however, there is ~20 cm of non-welded material above the welding unit. This must reflect in part, the incorporation of D5 material into the welding unit.

At two of the welded sections (3 and 5), there is a sudden onset of welding to a slightly welded grade without an intermediate tack-welded zone. The absence of such a transitional tack-welded zone suggests the onset of welding was triggered by an abrupt shift in conditions at the time of onset of welding rather than attainment of some critical value of loading. The sharp increase in welding grade is not coincident with changes of grain size or thickness. The observations suggest that an abrupt increase in accumulation rate could potentially be the key factor leading to onset of welding. Within D4, the vertical onset of welding is not accompanied by an increase in clast size, in fact generally there is a local decrease in grain size. Thus we infer that grain size is, at best, a second order factor facilitating welding and that potentially other factors such as local variations in accumulation rate and thickness of the overlying material may be more significant factors.

4.3. Case study 2: high W2 regional welding grades at section 6

Regional welding in the W2 welding unit is observed to fluctuate in both intensity and thickness along the northern rim. At the site of our second case study (section 6) (Fig. 9a and b) we observe the W2 welding unit forming a prominent ledge, which extends to the east and west of this section. This location falls within the second, or western, welding grade maximum for W2 (Fig. 9b). We use this section first to characterize the patterns and intensities of the W2 welding maxima on the northern rim, and second to contrast the welding characteristics of a welding maximum with those of the onset of welding. The thickness of W2 is variable (2 –17 cm) over a lateral distance of ~2 m, however this welding unit is always present with no reversals back to purely non-welded material. The upper and lower boundaries of this unit are sharp, with abrupt contacts to

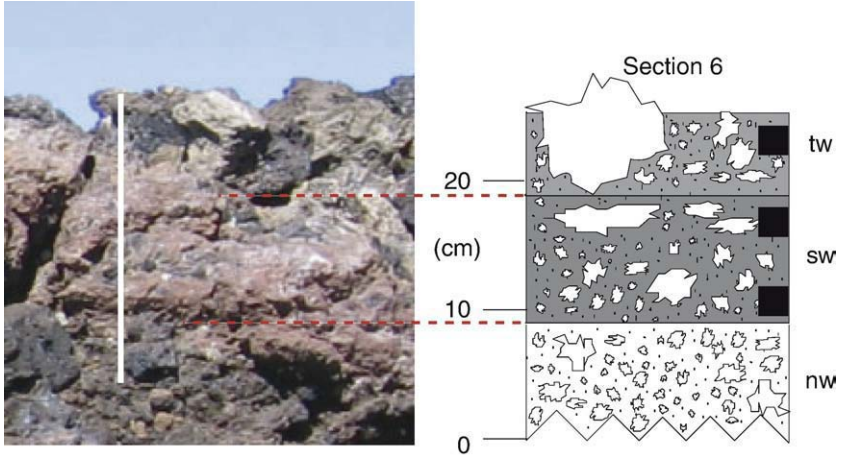

Fig. 13. Stratigraphic section and photograph of section 6 from W2: This profile was taken through the W2 unit at the western welding maximum.

Please cite this article as: Carey, R.J., et al., Contrasting styles of welding observed in the proximal Askja 1875 eruption deposits I: Regional welding, J. Volcanol. Geotherm. Res. (2008), doi:10.1016/j.jvolgeores.2007.11.020

Table 4a
Table of the welded and calculated pre-welding thicknesses for each zone within section 6. Using a calculated bulk density for the original non-welded D4 material (548 kg m^{-3}), and density measurements collected from each welded layer, calculations of the pre-welding thicknesses were made

	Section 6
Measured thicknesses (cm)	
Tack-welded	7
Slightly welded	10
Non-welded	9
Total (cm)	26
Total welded (cm)	17
Original thickness (cm)	
Tack-welded	14
Slightly welded	29
Non-welded	9
Total (cm)	52
Total welded (cm)	43
Thickness change (cm)	26
% Original thickness	50

an underlying non-welded lower D3 layer and an overlying zone of larger D5 clasts with sintered bases. The density values for regionally welded W2 are the highest collected from 10 sections measured along the rim. A measured profile at section 6 (profile III in Carey et al., in press) is 17 cm-thick, consisting of a basal 10 cm that is slightly welded, and an upper 7 cm of tack-welded material (Fig. 13). Non-welded D4 material is 9 cm-thick at the base.

Density measurements in the slightly welded zone are 1550 and 1620 kg m^{-3}. In the tack-welded zone, a sample yields 1120 kg m^{-3}. Average aspect ratios from the slightly welded deposits are only slightly larger than tack-welded deposits, 2.6:1 vs. 2.4:1. Within the welding unit there does not appear to be any systematic changes in grain size either vertically or horizontally along strike.

We have calculated the pre-welded thickness of the W2 unit. The present day total D4 thickness of section 6 (~26 cm) is only 49% of the inferred original thickness prior to welding, which represents a significant volume reduction (Tables 4a and 4b). The density measurements collected from this section are the highest of the whole dataset collected from W2 on the northern rim, despite its only moderate pre-welding thickness (52 cm).

4.4. Case Study 3: high regional W1 welding grades at section 7

Section 7 is located approximately 101 m to the west of section 6 (Fig. 9a and b). This location falls within one of the welding maxima (moderate welding) for W1 (Fig. 14; Tables 5a and 5b). We use this case study to characterize the patterns of the welding maxima in W1 and to compare the welding maxima present in W1 and W2. W1 extends as a continuous unit to the east and the west of section 7, with minimal thickness variations. The upper and lower contacts between W1 and non-welded material are fairly sharp and the high degrees of tack-welding in W1 allows it to protrude as a bench.

At the base there is 5 cm of non-welded D2 material, then W1 comprises five welded zones overlain by non-welded D3 deposits. The lowermost tack-welded zone (10 cm) has a density value of 1090 kg m^{-3}. It is overlain by a 3 cm-thick moderately welded zone with a density value of 1610 kg m^{-3}, and the average aspect ratio of lapilli in this zone is 4.9:1. It is overlain by a 10.5 cm-thick slightly welded zone (1340 kg m^{-3}, AR = 3.1:1) grading sharply into 5 cm of tack-welded zone (590 kg m^{-3} AR = 1.5:1). At this section, the present day thickness of W1 is 38.5 cm which, compared with the calculated pre-welding thickness of 69.8 cm, represents ~55% of the original thickness (Table 5a). Section 6 has a greater bulk reduction in volume than section 7 despite its smaller pre-welding thickness (52 vs. 70 cm) and lack of moderately welded deposits.

5. Interpretation

5.1. Summary characteristics of the welded and equivalent non-welded deposits

W1 and W2 are not restricted to the welding of purely coarse ejecta, but often comprise dominantly fine ash to medium lapilli. This has implications for eruption and emplacement mechanisms, in particular eruption styles, eruption temperatures and source vents. Irrespective of welding grade, the northern proximal exposures have the following features in common;

i) the welding grade can change over a short vertical interval without an obvious change in grain size.
ii) the onset of regional welding is usually sharp from underlying non-welded D2 or D4 deposits, often marked by an overhanging welded bench.
iii) generally tack-welded deposits characterize the top of the welding unit.
iv) the top of W2 is not necessarily coincident with the top of D4, and D5 bombs and clasts often penetrate into the welding unit.
v) W1 typically encroaches into original non-welded D3.
vi) the onset of welding is not coincident with an increase in grain size at all of the welded sections; instead at sections like 1, 3, and 5 there is actually a local reversal and decrease in the mean grain size.

5.2. Comparisons between W1 and W2

5.2.1. Vertical changes in welding density

The case studies have shown similar values for clast aspect ratio and density data in the two welding units. However, the

Table 4b
Density values (kg m^{-3}) used for the pre-welding calculations of section 6

Welding grade	Density kg m^{-3}
Tack-welded	1120
Slightly welded	1585
Non-welded	548

Please cite this article as: Carey, R.J., et al., Contrasting styles of welding observed in the proximal Askja 1875 eruption deposits I: Regional welding, J. Volcanol. Geotherm. Res. (2008), doi:10.1016/j.jvolgeores.2007.11.020

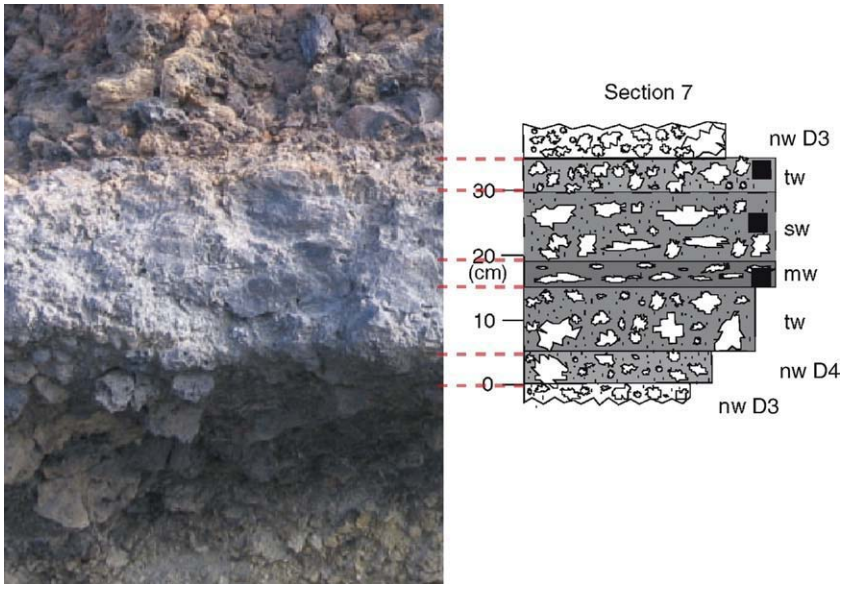

Fig. 14. Stratigraphic section and photograph of section 7 from W1: This profile represents the welding maxima in W1.

moderate welding grades observed in W1 are not observed in W2. We speculate that higher accumulation rates provide the insulation and heat retention required to achieve these moderate grades and is the dominant facilitating factor. However, a secondary role of loading, and hence insulation by the overlying D3 deposits potentially could have facilitated higher welding grades in W1. For case studies 2 and 3, the highest density measurements collected were from the mid-upper portion of the W1 and W2 units. One difference between the welding maxima of W1 and W2 is the relative shift to higher degrees of welding; i.e. at section 7 there is a sudden shift within the welding unit (between tack-welded and moderate welding) versus the less abrupt shift in W2 at the boundary between non-welded D4 and slightly welded W2. The W1 welding grades and densities are all higher than for W2; however, the overall reduction in volume is not greater than W2.

Table 5a
Table of the welded and calculated pre-welding thicknesses for each zone within section 7. Using a calculated bulk density for the original non-welded D4 material (548 kg m^{-3}) and density measurements collected from each welded layer, calculations of the pre-welding thicknesses were made

	Section 7
Measured thicknesses (cm)	
Non-welded	5
Tack-welded	5
Slightly welded	11
Moderately welded	3
Tack-welded	10
Non-welded	5
Total (cm)	39
Total welded (cm)	29
Pre-welding thickness (cm)	
Non-welded	5
Tack-welded	5
Slightly welded	26
Moderately welded	9
Tack-welded	20
Non-welded	5
Total (cm)	70
Total welded (cm)	60
Thickness change (cm)	31
% Original thickness	55

5.2.2. Lateral changes in welding density

The two welding units show very different aerial distributions for thickness maxima and welding grade (Fig. 9a and b). W1 has a more complex pattern, with reversible changes in thickness and welding along the region of continuous welding. In W1, the zones of higher welding grade are approximately correlated with increases in thickness of the unit; however, in two areas, X_2 and X_3 (Fig. 9a), the thickness of the unit can decrease to 20 cm without any change in welding grade. The sharp onset of moderate welding from tack-welding whilst maintaining a similar thickness is also interesting. In addition, the discontinuous western fringe to W1 can vary in thickness by up to 20 – 30 cm, and still maintain a similar welding grade. These factors together would suggest that the accumulation rate is the critical factor leading to increases of the welding grade. The short distances over which welding grade can change without changes in thickness would also suggest unsteadiness in the transport regime, leading to localized fluctuations of the accumulation rate.

Table 5b
Density values (kg m^{-3}) used for the pre-welding calculations in section 7

Welding grade	Density kg m^{-3}
Non-welded	548
Tack-welded	590
Slightly welded	1340
Moderately welded	1620
Tack-welded	1090
Non-welded	548

Please cite this article as: Carey, R.J., et al., Contrasting styles of welding observed in the proximal Askja 1875 eruption deposits I: Regional welding, J. Volcanol. Geotherm. Res. (2008), doi:10.1016/j.jvolgeores.2007.11.020

5.2.3. Physical changes accompanying welding

Volume loss during welding is accommodated by reduction of pore space in the deposit, both densification of the matrix and subsequently pumice clast flattening. The physical changes of density and pumice clast aspect ratios therefore can be compared with calculated reductions of original non-welded thickness.

In case study 1, we observe the highest flattening ratios within the slightly welded deposits at sections 1 and 3; however, the highest density measurements collected were from sections 3 and 5. The reduction in volume was greatest for sections 1 and 3. Case study 2, representing the W2 maxima, has similarly high values of density for slightly welded deposits, but it also has the smallest clast aspect ratios of all the case studies. The reduction of volume was the greatest at this section. Case study 3 had high densities and moderate aspect ratios, and the reduction in volume was intermediate between case studies 1 and 3. Thus it appears that in the 1875 regional welded deposits, aspect ratio is not a uniformly reliable indicator of either the onset or degree of welding and that the majority of the volume loss was accommodated by a reduction of pore space and densification of the matrix. At Askja, regional welding is principally a function of variable degrees of compaction and densification of the matrix.

5.3. Relationship between original thickness and welding grade

The original thicknesses of the welded sections in each case study does not seem to affect either a) the maximum welding grade attained, b) the maximum value of measured density or c) the highest aspect ratios of pumice. In addition, the maximum density and aspect ratios measured in each of the sections is in the mid to upper portion of the sections. This combination of thorough observations from seven sections suggests that welding was facilitated by other factors than simply loading.

In W1, the thickness maxima correspond with increases in welding grade from tack to slight welding (Fig. 9a). In addition the western thickness maximum corresponds with the zone of most intense welding (moderate welding) between 1160 and 1200 m from Víti. However in between these two maxima, we also see another lateral welding grade increase from tack to slight welding, with no obvious correlation to an increase in thickness. Table 6 describes the thickness variability for each welding grade observed in the continuous welding zone.

In W2, the onset of the slight welding from the eastern margin corresponds exactly to an increase in the thickness of the welding unit (Fig. 9b). However, as was the case for W1, the thickness can vary by +/− 10 cm on a local scale and there is no significant change in welding grade.

Table 6
Welding grades associated with the W1 and W2 welding units and the corresponding thicknesses observed for each welding grade

Welding unit	Degree of welding	Thickness range
W1	Tack-welding	0–30 cm
	Slight welding	10–30 cm
	Moderate welding	20–30 cm
W2	Tack-welding	0–20 cm
	Slight welding	20–30 cm

5.3.1. Implications

These data suggest that there is at best a broad relationship between welding grade and thickness. However, these data are more compatible with a scenario where local fluctuations in accumulation rate over short distance and time scales are the dominant factor. If the accumulation rate fluctuates such that some areas receive short-lived higher deposition rates, the observed broad relationship between welding grade and thickness could result.

5.4. Inferences from the patterns of welding

5.4.1. Sharp vertical changes in welding grade

The abrupt vertical change from non-welded to slightly welded grades within all W1 and some W2 sections, without a significant thickness of the overlying material, would suggest that the higher intensities are being induced by a process other than loading. In the 1875 regionally welded deposits, we commonly recognize sharp vertical changes of welding grade (e.g. Section 4.2). Jumps in welding grade occur in both units, but at contrasting points in the welding profiles. In W1 the jump is from tack to moderately welded, i.e., within the welding unit, whereas in W2 the shift is from non-welded to slightly welded without intervening tack-welding. This has implications for the timing within D2/W1, D4/W2 of increases of the accumulation rate. In D2 times, the initial accumulation rate must have been sufficient to facilitate low grades of welding prior to a sudden increase where moderate grades of welding were possible. In D4 times, the initial accumulation rates did not permit welding to occur. We suggest that rapid vertical changes in welding grade equate to shifts in intensity within each phase. The highest density samples were collected from the middle and upper zones of the W2 unit. Therefore in the absence of a significant thickness of D4 material above the slightly welded zone (<7 cm original thickness) it appears that the pre-welding thickness at section 6 did not have a significant effect on the final welding grade. All case studies also show that shifts in welding grade do not coincide with shifts in grain size.

5.4.2. Rapid and reversible lateral changes

It appears from case study one, where there are no obvious lateral shifts in grain size and a poor correlation of pre-welding thickness and welding grade, that thickness and grain size are not first order factors leading to the onset of welding. It seems instead that changes in eruptive conditions led to short-lived and local changes in the accumulation rate at some sections, which then led to both higher welding grades and greater thicknesses. What is interesting is that these fluctuations of accumulation rate are very localized; non-welded and welded sections can exist within less than 10 m of each other. This discontinuous pattern of welding onset over such short lateral distance scales, without increases in either grain size or total thickness suggests that heat loss was faster at some sections than others. This can be adequately explained by the lateral variability of the

Please cite this article as: Carey, R.J., et al., Contrasting styles of welding observed in the proximal Askja 1875 eruption deposits I: Regional welding, J. Volcanol. Geotherm. Res. (2008), doi:10.1016/j.jvolgeores.2007.11.020

accumulation rate throughout the period of deposition. These fluctuations occurred on very localized scales (<10 m) and must be explained in terms of processes of pyroclast transport, which also has implications for the eruption style. The welding maxima case studies (2 and 3) show less lateral variability in welding grade or thickness than seen for case study 1.

6. Discussion

6.1. Comparisons with other welded deposits

The 1875 welded deposits are quite distinct in terms of their inherent properties and the physical patterns of welding observed. Here we show five regional welded profiles from the 1875 welded deposits, and compare these with three welded fall deposits of Santorini and Mayor Island (Sparks and Wright, 1979; Houghton et al., 1985) and four profiles through well-known welded pyroclastic flow deposits (Fig. 15) (Sheridan and Ragan, 1976; Kamata et al., 1993; Quane and Russell, 2005; Sheridan and Wang, 2005).

The 1875 welded deposits have an almost symmetrical profile on graphs of normalized stratigraphic height vs. normalized density (ρ/ρ[DRE] (Fig. 15). In detail, the trend to higher density values is very uniform between profiles with a gradual increase to a central zone characterized by stable welding values, but with curves slightly displaced from one another in terms of absolute welding intensity (density) (Fig. 15). The uppermost portion of each profile is different between samples. In other welded fall units plotted in Fig. 15, the vertical profiles are generally similar with exception of Ruru Pass, which is the thickest of the welded fall deposits described here (7 m). However, the other fall units have higher densities than the 1875 profiles, almost consistently by 10–25% (Fig. 15). Welded pyroclastic flow profiles in comparison are dissimilar to those of the 1875 or other welded falls. The density values are much more uniform over the entire thickness, in contrast to welded fall deposits which show greater shifts in density values within a single section (Fig. 15). In addition, the welded flow deposits shown here and repeatedly commented on in the literature have their highest grades of welding in the lower third of the deposit, reflecting the enhanced role of loading (Sheridan and Ragan, 1976; Quane and Russell, 2005; Sheridan and Wang, 2005).

In terms of welding process, each of the fall units appears to require attainment of a critical rate of accumulation for welding to begin. The non-uniformity of the mid to upper portions of each section varies probably due to the heterogeneity of the welding material's characteristics (grain size, sorting, pyroclast temperature, etc.), and also the variability in factors such as accumulation rates. The layer-by-layer aggradation of fall material inhibits the formation of stable conditions of heat transfer, cooling and loading. This is the primary contrast with processes of welding and compaction in pyroclastic flow deposits.

6.2. Factors governing regional welding in the 1875 deposits

At all sites where we have studied W2, the welding patterns are similar: the onset of welding is characterized by slight welding grades some distance above the base of the stratigraphic unit; commonly, the highest density sample collected from each

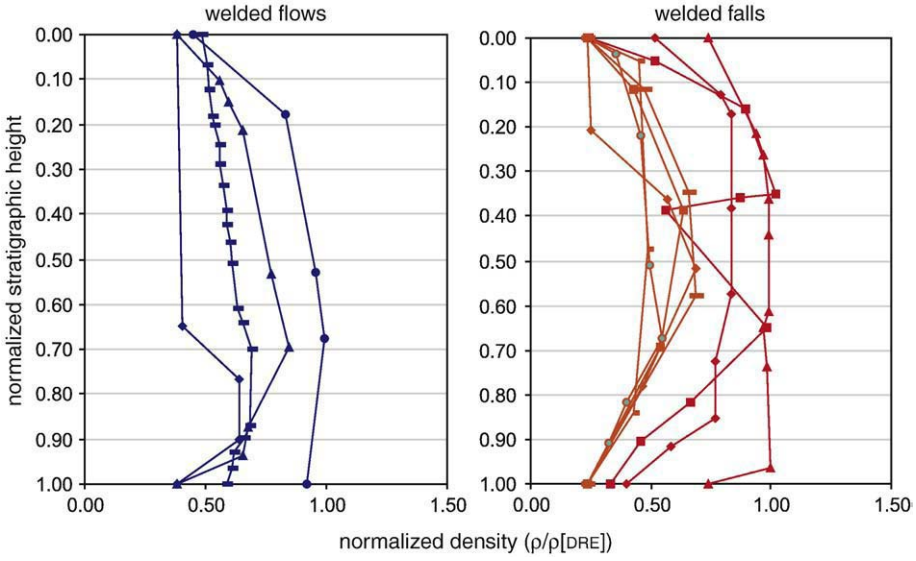

Fig. 15. Graphs of normalized density (ρ/ρ[DRE]) vs. normalized stratigraphic height. Graph on right represents density profiles through welded fall deposits. Five profiles through the Askja 1875 welded deposits are in orange and three other welded fall deposits are from Santorini (Thera = red squares, Therasia = red diamonds) (Sparks and Wright, 1979) and the Ruru Pass (red triangles) (Houghton et al., 1985). Graph on left shows four density profiles from welded flow deposits taken from the literature: Bishop Tuff (blue triangles) (Sheridan and Wang, 2005), Bandalier Tuff (blue rectangles) (Russell and Quane, 2005), Wineglass Welded Tuff (blue circles) (Kamata et al., 1993) and Ito Tuff (blue diamonds) (Sheridan and Ragan, 1976). Note the contrasting profiles between welded fall and flow deposits; in addition, the Askja profiles are displaced to lower density values with respect to the other fall deposits. (For interpretation of the references to colour in this figure legend, the reader is referred to the web version of this article.)

Please cite this article as: Carey, R.J., et al., Contrasting styles of welding observed in the proximal Askja 1875 eruption deposits I: Regional welding, J. Volcanol. Geotherm. Res. (2008), doi:10.1016/j.jvolgeores.2007.11.020

section is from the middle to upper parts of the unit. These observations, together with the rapid lateral shifts between welding grades regardless of overlying thickness in both W1 and W2, suggest that loading was not a first order factor facilitating welding during the 1875 eruption.

The three case studies from the northern rim strongly suggest that local accumulation rate is the dominant factor facilitating regional welding during both periods of welding. The similarities in the patterns of welding and density measurements taken from W1 and W2 maxima suggest similar general shifts in eruptive conditions during the two depositional periods (with second-order local fluctuations in rate of clast accumulation producing local variability in welding grade). Each unit experienced a rapid increase in mass flux of deposited material leading to higher accumulation rates and a jump in welding intensity. The switch in relative position of these jumps in welding grade has simple implications for the relative timing of the increase in the accumulation rate. However in contrast to the conditions during the emplacement of W2, the accumulation rate throughout D2/W1 deposition must have been sufficient enough to produce tack-welding.

6.3. Implications for eruptive style

6.3.1. Inferences from clast dispersal

The dispersal data for the D2 and D4 deposits are incompatible with their being derived from the full height of the 1875 Plinian eruption plume, estimated to be 26 km by Carey and Sparks (1986), as the thickness half distances for proximal Plinian falls of this intensity are typically 1 – 4 km (Pyle, 1989, Houghton et al., 2000). For comparison, thickness half distances for historical Strombolian and Hawaiian deposits are typically several tens of meters (Houghton et al., 2006). Thinning half-distances for D2 and D4 are of the order of 100–200 m, the only pyroclastic fall units of comparable geometry are those described by Houghton et al. (2004) for the 1912 Novarupta eruption and Sable et al. (2006) for the 1886 Tarawera eruption. In both cases the authors inferred these units to have incorporated large volumes of material shed by fountaining parts of the jet phase of eruption plumes, from heights of probably 1–4 km.

The comparison with Novarupta and Tarawera also permits some speculation about the positioning of the vents responsible for D2 and D4. The Novarupta exposures occur between 250 m and 1.5 km from vent (Fierstein et al., 1997; Houghton et al., 2004). The Tarawera deposits form a series of half cones between 500 and 600 m from the center of the 1886 craters. This is strong indirect evidence that the vent or vents responsible for D2 and D4 were probably within 1 km of the modern northern caldera rim. The E–W elongate geometry of both units is also difficult to reconcile with their resulting from eruptions from a single point source.

6.3.2. Inferences from clast cooling times

Cooling time calculated from Hort and Gardner (2000) for 2 cm pumices is 150 s and for a 5 cm clast 10 min. If D2 and D4 clast assemblages, with their high abundance of ash matrix are to retain sufficient heat to weld on deposition, the cooling times are much less than 2 min. This implies three things; first a high eruption temperature, second that the clast assemblage must not be in the air for an extended period and last, that the material must be covered quickly (high accumulation rates preventing heat loss). The transport time for 2 mm pumice shards falling at their terminal velocity from heights of 5 km is approximately 40–50 s (Wilson, 1972). Considering that the matrix of D2 and D4 subunits consists of between 20–40% ash, these particles must have fallen from heights much less than 5 km, probably $\ll 2$ km.

6.3.3. Variation of eruption intensity with time

It is difficult to assign intensities to the D2 and D4 fountaining vent(s). The sharp boundary between D1/D2 and D3/D4 observed in non-welded deposits (Fig. 4) suggests that the shifts in eruptive conditions were relatively sharp and the fountaining activity dominated the proximal environment in D2 and D4 times. However, in each instance, accumulation rates and, by inference, mass discharge rates were insufficient to immediately promote welding. The implication is thus that in both phases the intensity of activity increased with time. The pattern of welding intensity with time in W1 is also suggestive that maximum accumulation rates occurred relatively late in D2 times. Samples from the upper middle portion of welded W2 yield the highest densities suggesting high intensities at this time. The weakly defined upper boundaries to D2 and D4 suggest that the fountaining activity declined steadily over some finite period.

6.3.4. Stability and directionality of the fountains/jets

Section 4.1 illustrated the extreme lateral variability in pre-welding thickness of the original non-welded D4 deposits (up to a 45 cm change in vertical height over a 6 m distance). The irregular thickness data and the lack of a continuous pattern of increasing welding intensity at the eastern and western margins of the welding units suggests that on short lateral scales of a few tens of meters, accumulation rates varied considerably. We consider that this can only be associated with considerable variability in the pyroclast sedimentation rate either through episodicity or directionality of the fountains. This scenario is explored in detail in the companion paper (Carey et al., in press).

7. Conclusions

The case studies described above show that regional welding was possible during this sustained eruption only during periods of fountaining of ejecta from elevations well below the postulated height of the convective plume. However, accumulation rates had to reach a critical point at which significant heat retention could occur. Deposition along the entire northern rim was subject to an abrupt shift in eruptive conditions promoting jumps in welding state during both D2 and D4 times. Considering that the highest welding grades within W1 and W2 can occur with only $\sim<10$ cm of tack-welded material above, loading was not a determinant factor and high emplacement temperatures should also be considered as a first order control on welding. On a finer scale, changes in maximum welding grade on distance scales of tens of meters imply second order fluctuations in accumulation rate which we link to instability of

Please cite this article as: Carey, R.J., et al., Contrasting styles of welding observed in the proximal Askja 1875 eruption deposits I: Regional welding, J. Volcanol. Geotherm. Res. (2008), doi:10.1016/j.jvolgeores.2007.11.020

the fountaining jets. The process of welding in the 1875 deposits led to only moderate welding grades and much lower intensities than those described for other welded fall and flow deposits. The limited duration of the fountains and the progressive accumulation of the deposit did not permit higher grades of welding as observed in pyroclastic flows, which are rapidly emplaced and cool as a single isothermal unit.

Acknowledgements

This study was supported by NSF grants EAR-0310033 and EAR-0537459. Ármann Höskuldson participated in the field excursions and discussions and has contributed greatly to our understanding of the 1875 eruption. Field support was supplied by Tim Bowden (2004), Ben Sellers (2005), and Helena Buurman (2006). We acknowledge the generosity of our hosts, the Nordic Volcanological Center, Institute of Earth Sciences, University of Iceland, with scientific and logistical support, and in particular access to the Askja huts. We particularly thank Halldór Ólafsson and Eric Sturkell for their discussions and company in the field. We also wish to thank Lionel Wilson, Lucia Gurioli and Sarah Fagents for detailed thoughtful reviews of the manuscript.

References

Calderone, G.M., Gronvold, K., Oskarsson, N., 1990. The welded air-fall tuff layer at Krafla, northern Iceland: a composite eruption triggered by injection of basaltic magma. J. Volcanol. Geotherm. Res. 44, 303–314.

Capaccioni, B., Cuccoli, F., 2005. Spatter and welded air fall deposits generated by fire-fountaining eruptions: Cooling of pyroclasts during transport and deposition. J. Volcanol. Geotherm. Res. 145, 263–280.

Carey, S., Sparks, R.S.J., 1986. Quantitative models of fallout and dispersal of tephra from volcanic eruption columns. Bull. Volcanol. 48, 109–125.

Carey, R.J., Houghton, B.F., Thordarson, T.T., in press. Contrasting styles of welding observed in the proximal Askja 1875 eruption deposits II: local welding. J. Volcanol. Geotherm. Res. doi:10.1016/j.jvolgeores.2007.11.017.

Cas, R.A.F., Wright, J.V., 1987. Volcanic successions: Modern and ancient. Allen and Unwin, London. 528pp.

Duffield, W.A., 1987. Fire fountains of high silica rhyolite magma: a tin-rich aerosol? GSA meeting abstract.

Fierstein, J., Houghton, B.F., Wilson, C.J.N., Hildreth, E.W., 1997. Complexities of Plinian fall deposition at vent: an example from the 1912 Novarupta eruption (Alaska). J. Volcanol. Geotherm. Res. 76, 215–227.

Hackett, W.R., Houghton, B.F., 1985. Pinnacle Ridge Member, Whakapapa Formation: a welded airfall deposit from Ruapehu volcano, Taupo Volcanic Zone. N. Z. Geol. Surv. Rec. 8, 24–29.

Head, J.W., Wilson, L., 1989. Basaltic pyroclastic eruptions: influence of gas-release patterns and volume fluxes on fountain structure, and the formation of cinder cones, spatter cones, rootless flows, lava ponds and lava flows. J. Volcanol. Geotherm. Res. 37, 261–271.

Hort, M., Gardner, J., 2000. Constraints on cooling and degassing of pumice during Plinian volcanic eruptions based on model calculations. J. Geophys. Res. 105, 25981–26001.

Houghton, B.F., Bonadonna, C., Gregg, C.E., Johnston, D.M., Cousins, W.J., Cole, J.W., Del Carlo, P., 2006. Proximal tephra hazards: Recent eruption studies applied to volcanic risk in the Auckland volcanic field, New Zealand. J. Volcanol. Geotherm. Res. 155, 138–149.

Houghton, B.F., Wilson, C.J.N., 2000. Pyroclastic fall deposits. In: Sigurdsson, H., Houghton, B.F., McNutt, S.R., Rhymer, H., Stix, J. (Eds.), Encyclopedia of Volcanoes. Academic Press, San Diego, pp. 555–570.

Houghton, B.F., Wilson, C.J.N., Fierstein, J., Hildreth, E.W., 2004. Complex proximal deposition during the Plinian eruptions of 1912 at Novarupta, Alaska. Bull. Volcanol. 66, 95–133.

Houghton, B.F., Wilson, C.J.N., Weaver, S.D., 1985. The Ruru pass tephra, A peralkaline welded airfall tuff from Mayor Island. N. Z. Geol. Surv. Rec. 8, 30–36.

Inman, D.L., 1952. Measures for describing the size distribution of sediments. J. Sed. Petrol. 22, 125–145.

Kamata, H., Suzuki-Kamata, K., Bacon, C.R., 1993. Deformation of the Wineglass Welded Tuff and the timing of caldera collapse at Crater Lake, Oregon. J. Volcanol. Geotherm. Res. 56, 253–266.

Karhunen, R., 1988. Eruption mechanism and rheomorphism during the basaltic fissure eruption in Biskupsfell Kverkfjöll, north-central Iceland. Nordic Volcanol. Inst. Research Report 8802.

Pyle, D.M., 1989. The thickness, volume and grain-size of tephra fall deposits. Bull. Volcanol. 51, 1–15.

Quane, S.L., Russell, J.K., 2005. Ranking welding intensity in pyroclastic deposits. Bull. Volcanol. 67, 129–143.

Russell, J.K., Quane, S.L., 2005. Rheology of welding: inversion of field constraints. Bull. Volcanol. 67, 173–191.

Sable, J.E., Houghton, B.F., Wilson, C.J.N., Carey, R.J., 2006. Complex proximal sedimentation from Plinian plumes: the example of Tarawera 1886. Bull. Volcanol. 69, 89–103.

Self, S., Sparks, R.S.J., 1978. Characteristics of widespread pyroclastic deposits formed by the interaction of silicic magma and water. Bull. Volcanol. 41, 196–212.

Sheridan, M.F., Ragan, D.M., 1976. Compaction of ash flow tuffs. In: Chilingarian, G.V., Wolf, K.H. (Eds.), Compaction of coarse-grained sediments, II. Elsevier, Amsterdam, pp. 617–717.

Sheridan, M.F., Wang, Y., 2005. Cooling and welding history of the Bishop Tuff in Adobe Valley and Chidago Canyon, California. J. Volcanol. Geotherm. Res. 142, 119–144.

Sigurdsson, H., Sparks, R.S.J., 1978a. Lateral magma flow within rifted Icelandic crust. Nature. 274, 126–130.

Sigurdsson, H., Sparks, R.S.J., 1978b. Rifting episode in north Iceland in 1874–1875 and the eruptions of Askja and Sveinagja. Bull. Volcanol. 41, 1–19.

Sigvaldason, G.E., 1979. Rifting, magmatic activity, and interaction between acid and basic liquids: The 1875 Askja eruption in Iceland. Nordic Volcanol. Inst. Research Report 7903.

Sigvaldason, G.E., 2002. Volcanic and tectonic processes coinciding with glaciation and crustal rebound: an early Holocene rhyolitic eruption in the Dyngjufjöll volcanic centre and the formation of the Askja caldera, north Iceland. Bull.Volcanol. 64, 192–205.

Smith, R.L., 1961. Ash-flow tuffs: their origin, geologic relations and identification. US Geol. Surv. Prof. Paper vol. 366, 1–81.

Sparks, R.S.J., Wilson, L., Sigurdsson, H., 1981. The pyroclastic deposits of the 1875 eruption of Askja, Iceland. Phil. Trans. Royal. Soc. London 299, 241–273.

Sparks, R.S.J., Wright, J.V., 1979. Welded air-fall tuffs. Geol. Soc. Amer. Spec. Paper vol. 180, 155–166.

Stevenson, R.J., Briggs, R.M., Hodder, A.P.W., 1993. Emplacement history of a low viscosity, fountain-fed pantelleritic lava flow. J. Volcanol. Geotherm. Res. 57, 39–56.

Stevenson, R.J., Wilson, L., 1997. Physical volcanology and eruption dynamics of peralkaline agglutinates from Pantelleria. J. Volcanol. Geotherm. Res. 79, 97–122.

Thomas, R.M.E., Sparks, R.S.J., 1992. Cooling of tephra during fallout from eruption columns. Bull. Volcanol. 54 (7), 542–553.

Turbeville, B.N., 1992. Tephra fountaining, rheomorphism, and spatter flow during emplacement of the Pitigliano Tuffs, Latera caldera, Italy. J. Volcanol. Geotherm. Res. 53, 309–327.

Thordarson, T., Carey, R.J., Houghton, B.F., in preparation. Historical accounts of 19th and 20th century volcanic eruptions at the Askja volcano (Iceland) with a special reference to the 1874–1876 volcano-tectonic event.

Walker, G.P.L., 1971. Grain-size characteristics of pyroclastic deposits. J. Geol. 79, 696–714.

Wolff, J.A., Wright, J.V., 1981. Formation of the Green Tuff, Pantelleria. Bull. Volcanol. 44, 681–690.

Wright, J.A., 1980. Stratigraphy and geology of the welded air-fall tuffs of Panterlleria Italy. Geol. Rundsch. 69, 263–291.

Please cite this article as: Carey, R.J., et al., Contrasting styles of welding observed in the proximal Askja 1875 eruption deposits I: Regional welding, J. Volcanol. Geotherm. Res. (2008), doi:10.1016/j.jvolgeores.2007.11.020